Growth and Grazing: Optimising Dilution Rates for Nonlinear Functional Responses

A dissertation submitted for a Degree of Master in Mathematical Modelling in Biology at the University of Leicester

by

Alyssa Pennini

Supervised by
Dr. Andrey Morozov

September 6, 2017

Declaration

All sentences or passages quoted in this project dissertation from other people's work have been specifically acknowledged by clear cross referencing to author, work and page(s). I understand that failure to do this amounts to plagiarism and will be considered grounds for failure in this module and the degree examination as a whole.

Name:

Signed:

Date:

Abstract

The presence of nonlinear grazing by microzooplankton on phytoplankton populations creates challenges in obtaining appropriate data for accurate rate estimates through the dilution technique, specifically in regards to the number of dilutions included in the experiment as well as the levels of those dilutions. This research aimed to optimise the allocation of dilution rates to account for nonlinearity as well as to develop a new method to approximate the, normally unknown, functional response curve to improve upon current methods and models.

In doing so, this paper demonstrates that a computational approach using the 4^{th} order Runge-Kutta method as well as constrained and unconstrained nonlinear optimisation is preferential to other approximated methods, especially in the necessary examination of multiple functional response curves. The results of the preliminary new method indicated that the inclusion of multiple high dilution samples (≤ 0.2), with at least one very highly diluted sample (≤ 0.05), provides minimal error for both the parameter estimates as well as the associated functional response curve in comparison to the known true response.

Therefore, this preliminary new method, though in need of refinement, shows promise as a tool to enhance the dilution technique method as well as to improve the progress and development of current plankton models for estimating the grazing rate of microzooplankton.

Acknowledgements

I would like to express my gratitude to my tutor and supervisor, Dr. Andrey Morozov, for his support, advice and guidance throughout the duration of this project. I would also like to acknowledge the contribution of Qian P. Li, Peter J.S. Franks and Michael R. Landry as their paper "Recovering growth and grazing rates from nonlinear dilution experiments" provided the foundation and source of data for this research project. Finally, I would like to thank my mother for her continued support and understanding, despite being an ocean away.

Table of Contents

Chapter 1 – Introduction

Mathematical biology and ecology attempt to describe and explain the natural world and various phenomena in an abstract or theoretical framework, translating complex behaviours into more simplified mathematical equations. [1: p.1] The resulting equations, though simplified in relation to the true biological or ecological processes, are still complex in terms of mathematical theory and analytical ability. [2: p.3-4] Therefore, scientists and researchers use mathematical modelling to focus on the most important and relevant parameters regarding their hypotheses and frequently employ computational methods to simulate the results.

One of the major areas of interest is the study of population dynamics whereby research is conducted in order to understand the factors contributing to the increase and decrease of populations over time. This includes the study of all species, from the largest of mammals down to the most minuscule microscopic organisms. Some of the smallest organisms are of specific interest to those studying aquatic ecology and there has been a continued focus on the ecological modelling of plankton populations and dynamics. Recent interest concerning plankton dynamics specifically revolves around the estimating of microzooplankton predation rates and their impact on phytoplankton populations, the relevance of which is due to the greater importance of phytoplankton in marine ecosystems.

As the foundation of the oceanic food chain, phytoplankton play a critical role in the well-being of not only the entire marine ecosystem but the planet as a whole. Though tiny organisms, their size belies their importance as phytoplankton are a source of food for most aquatic creatures and are primary producers of energy through the process of photosynthesis. [3: p.S17-S18] As the plants of the aquatic environment, phytoplankton serve as the direct food source for herbivorous zooplankton and then indirectly for omnivorous zooplankton and others as they travel up the food chain. [4: p.R482] Therefore, understanding and possibly predicting, the growth and mortality rates of phytoplankton allow for the study and modelling of the greater marine ecosystem.

FIGURE 1 –PLANKTON ROLES IN THE OCEAN FOOD CHAIN AND CARBON CYCLING [3: P. S20]

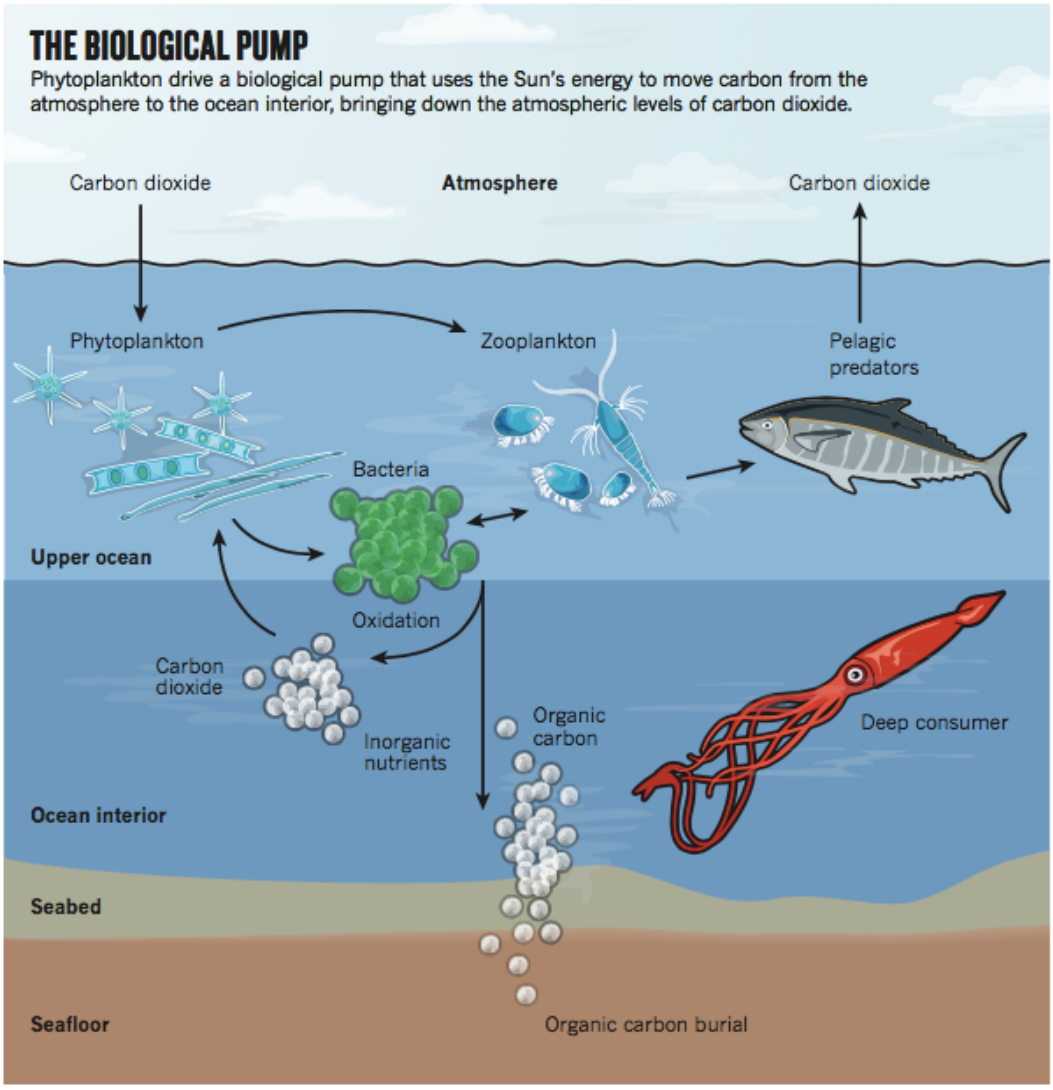

In their other role, phytoplankton are the most efficient primary producers given that they "are responsible for about 45% of global annual primary production" [4: p.R478], though they account for a tiny fraction of the total photosynthetic biomass on Earth. [3: p.S19] In this capacity, phytoplankton are important in regulating and contributing to the planet's carbon cycling as illustrated in Figure 1. In fact, without their presence, global warming and climate change would have greatly surpassed the current problematic levels.

Given the importance of phytoplankton in the marine ecosystem, it is imperative that the intricacies of their dynamics are further understood. More often than not, this takes the form of obtaining accurate growth and mortality rates of phytoplankton in different environments. In addition, consideration needs

to be made for the dynamics of the predators, specifically in regards to the microzooplankton. Of particular interest is accurately estimating the microzooplankton grazing rate or the rate at which the microzooplankton consume their phytoplankton prey. However, this is a task that is easier said than done.

Gathering data on plankton populations requires the completion of field, or *in situ*, experiments in various areas. However, as the majority of the planet is covered in water, there are many different aquatic environments to consider, some more accessible than others, which creates an additional challenge in obtaining robust data sets. The field experiments are also a time and labour intensive process that tends to, presumably, require sufficient funding to complete.

The actual obtainment of the data requires the completion of multiple experiments, typically conducted using the dilution technique. Though the technique requires little manipulation of the plankton [6: p. 284], it is not a particularly efficient process. Two specific shortcomings of the technique are the choice of the dilution levels as well as the number of dilutions included in the experiment. These issues have become more glaring flaws with the acknowledgement of the possibility of nonlinear functional responses which describe the predator's rate of consumption as a function of prey density. [5: p.385] Therefore, the dilution technique, which originally assumed a linear functional response, may not always garner accurate results due to variability within the experiment setup. [6: p.286]

In an effort to minimise some of these issues associated with the dilution technique, and improve overall accuracy and efficiency, the use of computational methods and numerical simulation have been employed in the development of a method for determining the optimal dilution rates for the enhancement of field experiments.

1.1. Background and Purpose

For many years only larger zooplankton, such as mesozooplankton, were modelled as their constant density and size allowed for relatively easy experiments and data collection. [4: p.R482] The singling out of the smaller zooplankton, specifically microzooplankton, and their grazing impact on

phytoplankton populations began in the 1980s due to the unknown significance of microzooplankton grazing to the microbial food web as shown in Figure 2. [7: p.75]

FIGURE 2 – ILLUSTRATION OF THE MICROBIAL LOOP [8]

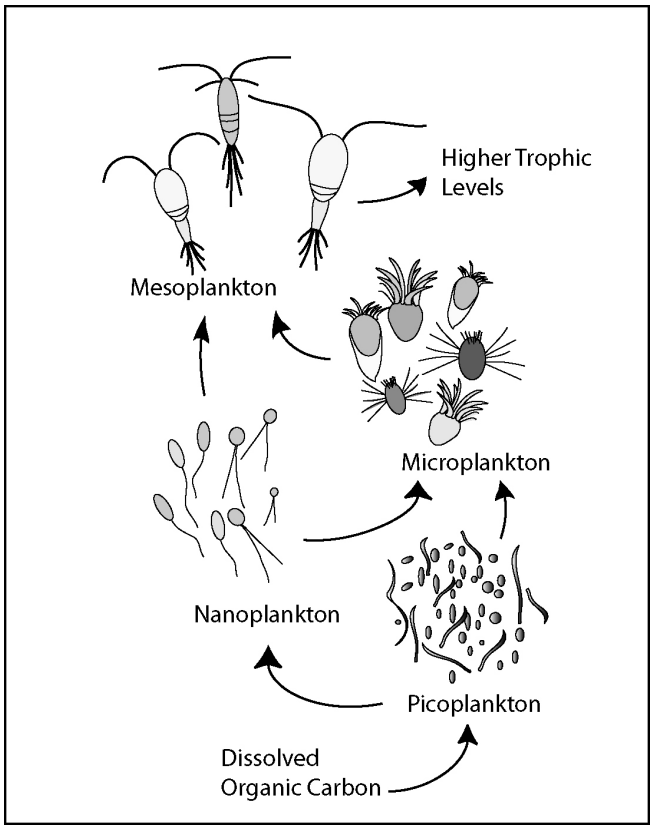

With their small size and similar growth rate to phytoplankton, microzooplankton dynamics are tightly coupled to that of their prey. [7: p.77] This creates challenges with regards to model development which requires the separation of the predator and prey populations to determine accurate rate estimates. The answer to this challenge is the dilution technique, developed by Landry and Hassett in 1982, which has subsequently been used in many studies in the intervening years. [6]

One of the original assumptions of the dilution technique was that the grazing functional response by microzooplankton was linear. [6: p.286] Over the years, contradictions to this assumption have been observed and it is now acknowledged that nonlinear functional responses are a likely possibility. However, that acknowledgement brings with it a set of challenges as the analysis of nonlinear curves is not as straightforward as with linear functions. Therefore, many studies have worked to improve both the dilution technique itself as well as model development and analysis.

One of the more recent studies was conducted by Li et al. titled, "Recovering growth and grazing rates from nonlinear dilution experiments." The objective of the research was to develop a theoretical method to estimate the growth and grazing rates from dilution experiment data. [9: p.2] In order to achieve this goal, the focus rested on simplifying and parameterising the first-order differential

equation describing plankton dynamics utilising a Holling Type II functional response curve using field experiment data.

$$\frac{dP}{dt} = \mu P - g_{max} f(P) Z \quad (1)$$

As the differential equation (1) representing the dynamics between the phytoplankton and the microzooplankton cannot be solved analytically, the authors employed Picard iteration to approximate a solution in the form of a mathematical equation. The resulting simplified model requires three parameters in addition to the dilution rate. [9: p.4]

$$\varepsilon_d = \mu - D\left(\frac{1+\frac{P_0}{K}}{1+D\frac{P_0}{K}}\right)\overline{m} \quad (2)$$

Using nonlinear optimisation of a cost function, specifically the minimisation of the sum of the squared residuals, the model (Eq. 2) was fitted to the multi-treatment experimental data resulting in the estimation of the optimal parameters for the phytoplankton growth rate (μ), the half-saturation constant (K) and the mean grazing rate ($\overline{m}$). The model was then modified in order to estimate the parameters when only 2-treatment dilution experiments have been conducted. [9: p.5] This is necessary as nonlinear grazing cannot be accurately estimated using 2-treatment dilution experiments.

With their study and findings as a starting point, this paper seeks to improve upon their method by capitalising on computational methods and numerical simulation to hopefully enhance field experiments and progress the development of ecological models. The research first focuses on the method of solution for the original differential equation (1) using multiple functional response curves. The second focus centres on optimising the allocation of dilution rates. Lastly, the research attempts to develop a method to approximate the functional response curve as it is normally an unknown factor.

1.2. Aims and Objectives

Originally, when microzooplankton grazing was assumed to be a linear function of phytoplankton density, there were no drawbacks in choosing any two dilution rates as that would be sufficient to perform a linear regression. However, there exists a challenge in determining the optimal number of dilution treatments

to perform as well as the best rates to achieve the most accurate estimates when nonlinear grazing is considered.

Therefore, the aim of this project is to improve the efficiency and accuracy of the dilution experiments by optimising the allocation of dilution rates. This should produce more accurate estimates for both the phytoplankton growth and microzooplankton grazing rates, especially in the case of nonlinear grazing.

To accomplish this, the 4^{th} order Runge-Kutta method is used in solving the differential equation before employing both unconstrained, for the parameters, and constrained nonlinear optimisation for the allocation of dilution rates. Numerical simulation also plays a critical role in determining the optimal dilution rates as well as creating the new method concerning the functional response curve. Finally, in regards to the functional response curve, the Holling Type II is the primary curve, however, three others, Holling Type I, Ivlev and hyperbolic tangent, are also considered and compared.

1.3. Assumptions and Limitations

The main assumption regarding this research is that the microzooplankton growth rate remains constant at zero throughout the experiment incubations. However, the implementation of the Runge-Kutta method to solve the differential equations allows for the testing of this assumption by fixing other parameters. In addition, linear regression is not performed as the grazing response is assumed to be nonlinear.

A second assumption is the general shape of the nonlinear dilution data as observed in the Li et al. paper. The shapes of the four data cycles remain consistent throughout this research and the simulated data is created utilising proportional noise, therefore there are no significant deviations such as increases at low dilution levels.

In regards to limitations, the research in this paper is restricted by the lack of the original raw data analysed by Li et al. In fact, this is a common limitation in plankton modelling and it inhibits the accurate estimation of model parameters. [10: p.694, 11: p.1304] The only other limitation in regards to this project is time. With four data sets, the consideration of four functional response curves and available computing power, the three additional functional response curves (Ivlev,

hyperbolic tangent, Holling II) are only considered for parameter optimisation, however the creation of the computer programs means that it would not be difficult to test and experiment with the other curves.

1.4. Hypothesis and Summary

The purpose of this research is to improve the modelling of microzooplankton grazing on phytoplankton populations in four separate forms. The first seeks to illustrate that computational and numerical methods are advantageous in their efficiency and accuracy over their approximated counterparts. The second will show that it is imperative to consider, in depth, multiple functional response curves in not only how well they fit they fit the data, but also the implications of the functional response itself. The third provides evidence for the optimal values for a certain number of dilution rates, specifically regarding the inclusion of at least one highly diluted sample. Finally, the fourth attempts to create a method that produces the optimal dilution rates to minimise the functional response error when the functional response curve is unknown.

Chapter 2 – Literature Review

2.1. History of Modelling Plankton Dynamics

The first and most famous mathematical model of predator-prey systems was developed separately by Alfred Lotka in 1925 and Vito Volterra in 1926. [12: p.54] The system of equations Lotka and Volterra developed consist of two coupled first-order differential equations, one describing the rate of change of the prey population density and the other, the rate of change of the predators. The system takes the general form:

$$\frac{dP}{dt} = (a - cZ)P, \ \frac{dZ}{dt} = (bP - d)Z \tag{3}$$

where $\frac{dP}{dt}$ represents the rate of change of the prey and $\frac{dZ}{dt}$ describes the rate of change of the predator. The terms P and Z represent the prey and predator densities, respectively, and a, b, c and d are constants. [7: p.70]

While the system of equations is a remarkable achievement, there exist critical assumptions that make the model unrealistic in describing the natural world. The assumptions are as follows:

1. "No other factors are considered significant with regards to the population dynamics
2. The prey grows and predator dies off exponentially in the absence of the other
3. The functional response of the predator is linear in regards to both the prey and the predators
4. Every prey death contributes identically to the growth of the predator population" [12: p.54-55]

However, as the relationship between two species in the natural world likely is not described by a linear function, the Lotka-Volterra equations are not the most accurate, but they do provide a useful foundation for adaptation. A common modification to the system of equations is in the choice of functional response curve which describes the predator per capita rate of consumption as a function of prey density with an upper limit of 1. [5: p.385] There are many different types of functional response curves, the most famous of which are attributed to the work of C.S. Holling. [1: p.79, 5: p.385] The three functional

response curves that bear his name are listed in Table 1 and illustrated in Figure 3.

TABLE 1 – HOLLING TYPE FUNCTIONAL RESPONSE CURVES

Holling I	$f(P) = \begin{cases} \frac{P}{2K} , & P < 2K \\ 1 , & P \geq 2K \end{cases}$
Holling II	$f(P) = \frac{P}{K + P}$
Holling III	$f(P) = \frac{P^2}{K + P^2}$

FIGURE 3 – HOLLING TYPE I, II, AND III FUNCTIONAL RESPONSE CURVES [1: P. 110]

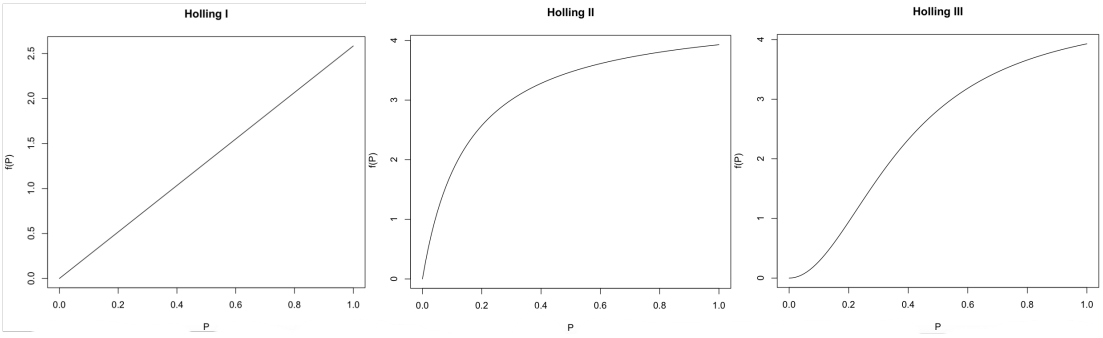

The Holling I curve is a simple linear response that does not include saturated grazing, but it can be transformed into a piecewise linear response that accounts for saturation. The Holling II curve is a concave response which eventually levels off as grazing becomes saturated, however, it has a destabilising effect due to predator inefficiency at high prey densities. On the other hand, the Holling III response is a sigmoid curve that not only incorporates saturation effects but also predator efficiency, producing a stabilising effect specifically at low prey densities. [1: p.80]

While being able to indicate a potential functional response curve from a raw dilution plot is possible, the development of a model requires the consideration of more than one curve. In addition, further examination is necessary as different functional response curves can fit the data equally well yet have significant differences specifically in the functional response.

The study of plankton dynamics has been a specific area of interest since 1939 when Richard Fleming adapted the Lotka-Volterra equation describing the

rate of change in the prey population to plankton dynamics, taking the form: [7: p.70]

$$\frac{dP}{dt} = (\mu - g)P \tag{4}$$

In the case where $g = cZ$, c being the clearance rate and Z the zooplankton biomass, the equation is equivalent to the Lotka-Volterra model. [13: p.745] The model has few terms and was only concerned with the growth and grazing rates of phytoplankton. However, Fleming acknowledged that there were a number of ways to adapt and modify the simple equation to obtain more realistic results. [7: p.70]

Fleming was proven right when, in less than a decade, his work was used as the basis for four models that became fundamental in the study of plankton ecology. During the years 1946 to 1949, biological oceanographer Gordon Riley developed both the first biological-physical and biological-chemical-physical models of plankton dynamics, as well as the first model for zooplankton dynamics and a model describing the nutrient-phytoplankton-zooplankton-carnivore food chain. [7: p.71-72] However, these realistic changes and adaptations resulted in complex nonlinear equations that required the use of numerical methods to solve, as analytical methods were intractable. Even so, the numerical methods used to approximate the solutions were complex and time intensive to complete by hand. [7: p.72]

The complexity challenge was soon met by technological advances and the introduction of the computer. With computational time no longer an issue, biologist John Steele was able to make great strides in the study of plankton dynamics beginning with a modification of Riley's food chain model in 1958. He also used technological innovations to his advantage by focusing on the sensitivity analysis of existing models to derive additional insight for new hypotheses. [7: p.73]

By the mid-1970s, Steele determined that before more progress could be made on phytoplankton dynamics, the focus needed to shift to studying and understanding the predators, namely zooplankton, in more detail. With the increased use of technology, more complex models were developed to target various intricacies of community structure such as demographics and biomasses. [7: p.73] Continuing on this line of investigation led oceanographer Bruce Frost to

ultimately show that present methods could not retrieve accurate results when grazing only occurred due to smaller zooplankton, namely microzooplankton, and further study needed to address this issue. [7: p.75]

As it became more apparent that the study of microzooplankton would be necessary to further the progress on plankton dynamics, it required a method to collect data on the microscopic predators. Therefore, in 1982, the dilution technique was developed by Landry and Hassett to address this issue. The technique, which is still the most common method of estimating microzooplankton grazing, includes diluting raw seawater samples at varying rates and then leaving the diluted samples in *in situ* conditions for a length of time, typically a day. [6: p.284-285] The technique has been modified and refined over the years depending on the hypothesis being tested in the experiment.

2.2. Dilution Technique: From Linear to Nonlinear Grazing

The dilution technique is popular due to its simple procedure as well as the limited manipulation of the sampled organisms. [6: p.284] However, the technique originally revolved around four important assumptions:

1. "Growth of phytoplankton is not directly affected by other phytoplankton
2. The probability of phytoplankton cell being consumed is a direct function of the rate of encounter of consumers with prey cells
3. Change in density of phytoplankton over time is exponential, and
4. Microzooplankton grazing is a linear response to phytoplankton density" [6: p.284]

Due to the assumption of a linear grazing response, the developers of the technique acknowledged that multiple dilutions could be used, but only a minimum of two was necessary, as only two points are required in fitting a straight line to the observed data. From the resulting analysis using linear regression, the grazing rate is determined by the negative slope and the phytoplankton growth rate is found at the Y-intercept of the regression line. [6: p.284]

The linear assumption is, presumably, based on the Lotka-Volterra equations and their assumption of linearity. In hindsight, it may seem short-sighted, but it does make sense that the authors would include simple assumptions in order to determine if the technique is, at the very least, a valid approach in a

limited theoretical sense. The problem comes when continuing to limit the possibilities, especially when studying the natural world which rarely adheres to simple assumptions.

One of the first to challenge these assumptions was Charles Gallegos in 1989 when he considered the possibility that microzooplankton grazing is not linear. In comparison to Landry's two-point dilution technique, Gallegos carried out modified 3-point dilution experiments with the resulting data plots indicating the presence of nonlinearity. [14: p.27] The 3-point experiments were also compared to various 2-point dilutions with the results showing that the higher the dilution rate, specifically greater than or equal to 95% (0.05) in the 2-point experiments, the closer the results were to the 3-point methods. On the other hand, the closer the dilutions were to 50%, the lower the parameter estimates in comparison to the 3-point experiments. [14: p.28]

Building upon the results obtained by Gallegos, a study in 1992 by Evans and Paranjape focused on analysing the issue of precision estimates in the case of nonlinear functional response. Unlike Gallegos, they considered the assumption that grazers respond continually to a varying phytoplankton density. In allowing this assumption, they accounted for curvature over the entire interval instead of a linear or linear piecewise functional response. [15: p.286]

In response to the research by Evans and Paranjape, Landry et al. modified the dilution technique in 1995 to account for some of the criticisms regarding the original assumptions. In analysing the findings of others, they determined that it would be best to modify the technique by adding nutrients to dilution samples and using fluorescently labelled bacteria to independently trace microzooplankton grazing activity. They argued that these refinements would improve results by accounting for potential changes in microzooplankton densities that had otherwise not been accounted for. [16: p.55]

By Landry and Hassett acknowledging a nonlinear grazing response, and continued observance of nonlinear data [17: p.427], it became apparent that the results of experiments offered more questions than answers. Subsequent studies focused on attempting to explain the presence of nonlinearity, and in doing so, confirm the continued validity of the dilution technique. [20: p.54] Two studies focused on the physical aspects of the dilution technique, namely the effect of

dilution itself on microzooplankton dynamics [18] as well as the effects of the nutrient amendment and enrichment. [19] Others specifically investigated the feeding behaviour and kinetics of the microzooplankton [13,20] as well as the possibility that assumed constants, namely grazing [21] and half-saturation [22], were more variable than constant.

The general consensus concluded that there was still much that was unknown about the specifics regarding microzooplankton community and grazing dynamics. In addition, the dilution technique was determined to still be valid regarding nonlinear functional responses, however, many researchers recommended steps to be taken to limit inaccuracies. These recommendations include at least one, preferably more, highly diluted samples from which to determine the phytoplankton growth rate [14,15,17,18,20] as well as using duplicates if conducting 2-point dilution experiments. [23: p.5]

Gallegos' research also introduced the first alternative to a linear functional response with the Holling I curve. [14: p.28] It is an appropriate choice as its piecewise linear formula differs only by including the possibility of saturated feeding. A more extensive analysis of the suitability of this curve was performed by Redden et al., who argued that this curve is a better compromise than other curves when faced with nonlinear data due to its relatively easy interpretability as well as its tractability. [24: p.28-29] Instead of relying on numerical methods as Gallegos did with the 4^{th} order Runge-Kutta method, Redden et. al showed that the equation can be solved analytically. [14: p.28, 24]

However, the choice of nonlinear functional response should not be restricted to the simplicity of the Holling I curve. The acknowledgement that microzooplankton grazing is possibly nonlinear opens up a variety of possible models, none of which are considered inherently 'correct'. [15: p.286] This has been illustrated over the years as both the Michaelis-Menton and hyperbolic tangent curves have been studied as well as the Holling II, Holling III and Ivlev functions. [15: p.286, 25: p.63] Therefore, this requires more experimentation and simulation with various models before finalising the best fit.

Even beyond experimentation, model fitting and selection require a measure of common sense, the consideration of the greater context and the practicality of the interpretation. There must be a balance in ecological modelling

between the mathematical and biological perspectives, especially in regards to the use of statistics. Though the general consensus in statistics is that the simple model is more often better, it is important to consider how a model will be used and its implications when choosing between a simple or more complex model. [15: p.288-289] It is also never advisable to limit selection to a single, or simply the linear, model, as additional, more complicated models could prove to be a better fit for both the data and interpretation.

Chapter 3 – Methods

3.1. Data

3.1.1. Data Collection

The main limitation for this project is the lack of access to the full datasets used by Li et al. and, therefore, without the raw data, estimations are used based on the plots included in their paper. This provided their summary of four multi-treatment dilution experiments for nonlinear fitting exercises, relying on the assumption that the phytoplankton and zooplankton biomasses were accurate. Their estimations for the phytoplankton growth and mortality rates, as well as the half-saturation constant, are used for comparison purposes between their approximations and the resulting differential equations as well as the starting point for the nonlinear optimisation of the estimated parameters. Those values are available in Appendix C.

FIGURE 4 – LI ET AL. DILUTION PLOTS WITH APPROXIMATION CURVES [9: P. 7]

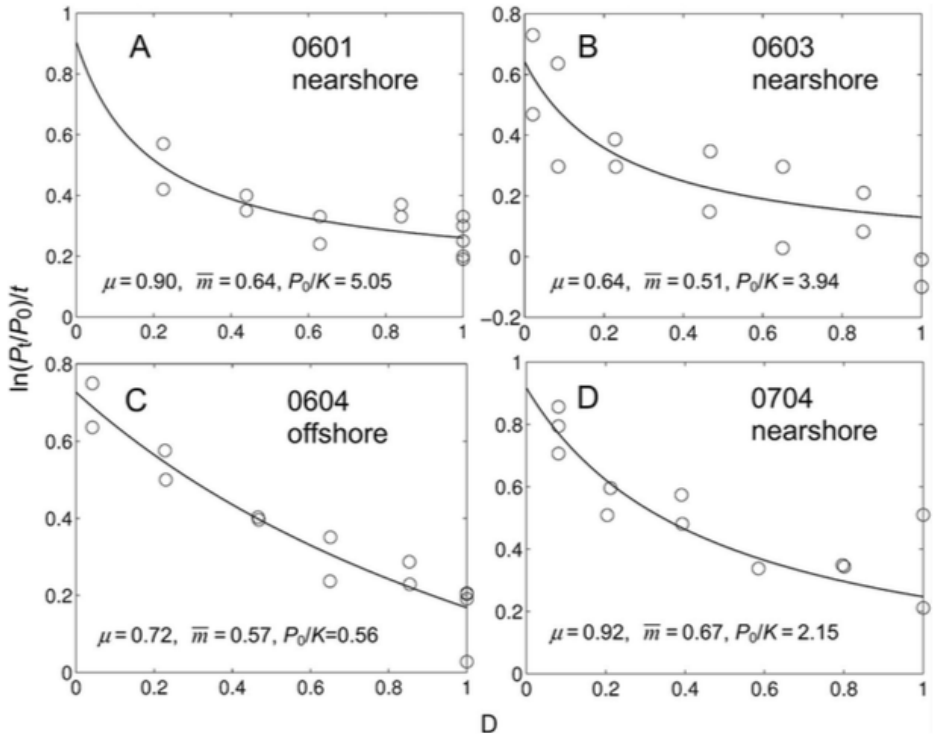

Fig. 4. Fitting the nonlinear model Eq. 23 to the 1-d multi-treatment dilution experiments in the California Current Ecosystem for Cycle 0601 (**A**), Cycle 0603 (**B**), and Cycle 0604 of the 2006 cruise (**C**) and Cycle 0704 of the 2007 cruise (**D**). *P* and *K* are in units of μM nitrogen.

In addition, the plots of fitting the nonlinear model for each of the four cycles provided data points for net growth as a function of dilution rate. With these

plots, shown in Figure 4, as the only access to the data needed for calculating the fit of the model, the data points need to be estimated. Taking screenshots of the plots from the paper, the package 'digitize' is used in the R software to extract the data points in the plot. Importing the plot into the R console, the digitize package allows for the marking of both the x- and y-axis bounds as well as each of the data points. With the additional input of the correct values of axis bounds, the package calibrates and returns approximations of the x and y values for each of the data points. [26: p.2-4]

With these approximated data points, the plots are recreated to ensure the process calculated appropriate and reasonable estimations. As the plots are virtually the same, the approximated data points are then utilised for the remainder of the project.

This still only provides limited data with 13 data points for cycle 0601, 14 points for cycles 0603 and 0604 and 12 points for cycle 0704. There are two points for cycle 0603 that contain negative net growth at the dilution rate of 1. These points are considered outliers and, therefore, are removed to provide more accurate model results. As an alternative, the negative values are also changed to 0 and the methods of parameter optimisation are applied to that set as well. The resulting data table and alternative results are available in Appendix C.

3.1.2. Data simulation

While observed data is only necessary to determine the optimal parameters for the phytoplankton net growth rate, the half-saturation constant and the maximum grazing rate, the majority of this research relies on simulated data with added random noise. The simulated data are created by solving the differential equation utilising the optimal parameters at varying rates of dilution. Noise is then added to the final simulated values at the same level for each rate of dilution which results in proportional noise across the entire dilution interval.

The noise level for this project consists of an interval 25% above and below the simulated data points. This is accomplished by using a normal distribution with the simulated values as the mean and a third of the 25% as the standard deviation given that 99% of values fall within three standard deviations of the mean. [27]

FIGURE 5 – EXAMPLE OF DATA SIMULATION

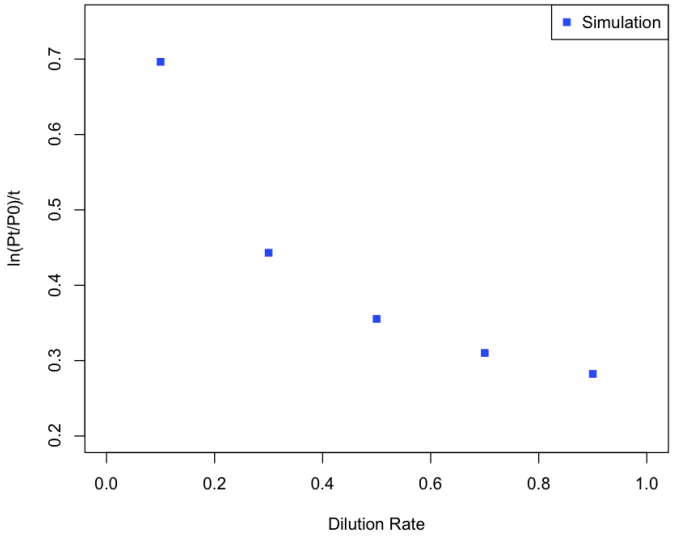

For example, Figure 5 depicts the simulated points for the dilution levels 0.1, 0.3, 0.5, 0.7 and 0.9 using the parameters from cycle 0601.

FIGURE 6 – EXAMPLE OF ADDING NOISE TO DATA SIMULATION

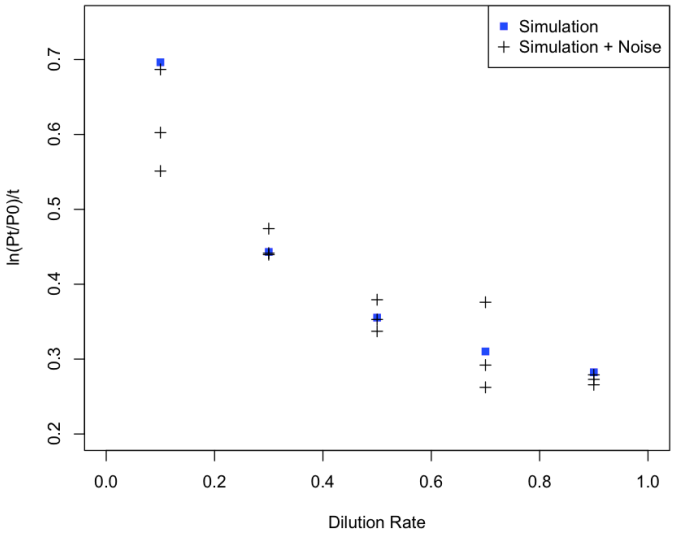

Noisy data are calculated for each dilution rate three times as depicted by the black crosses in Figure 6.

FIGURE 7 – EXAMPLE OF FINAL DATA SIMULATION WITH NOISE

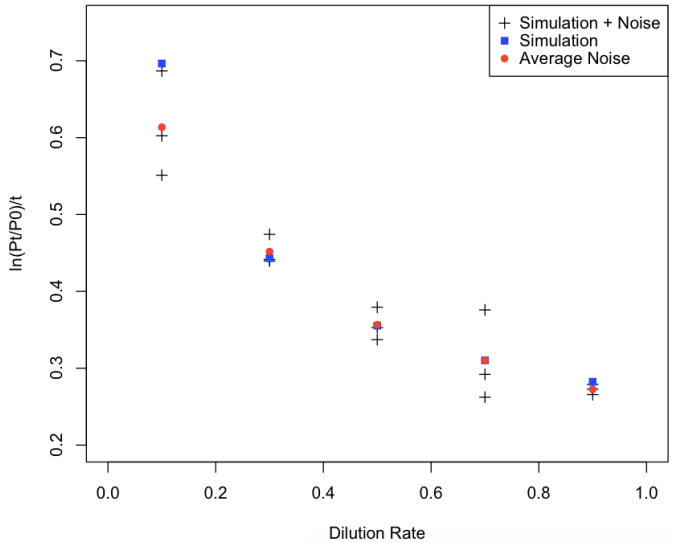

The three noisy data points are then averaged to determine the final noisy simulated data points that will be used in other tasks. Those final values are shown in Figure 7 as the red dots.

3.2. Runge-Kutta Method

The research in this paper centres around the solution of the ordinary differential equation describing plankton dynamics with a nonlinear grazing functional response. The general equation, first shown in the introduction, takes the form:

$$\frac{dP}{dt} = \mu P - g_{max} f(P) Z$$

where *f(P)* is substituted for the choice of nonlinear grazing functional response. The functional response curves that are examined in this research are listed in Table 2. As is the case with many mathematical models representing biological and ecological systems, the integration is too complicated for a closed-form, or exact, solution. With analytical methods unusable, it is necessary to turn to numerical analysis and methods in order to find an approximation to the solution.

TABLE 2 – NONLINEAR FUNCTIONAL RESPONSE CURVES

Holling Type I	$f(P) = \begin{cases} \frac{P}{2K} , & P < 2K \\ 1 , & P \geq 2K \end{cases}$
Holling Type II	$f(P) = \frac{P}{K + P}$
Ivlev	$f(P) = (1 - e^{-P/K})$
Hyperbolic Tangent	$f(P) = \tanh \frac{P}{K}$

One common approach, as employed by Li et al. in "Recovering growth and grazing", is to find an approximation via the Picard iteration method that results in a simplified mathematical equation. Picard iteration is built upon the method of integration which has to occur at each iteration, with the number of iterations depending on the desired level of accuracy. [9: p.3; 28]

As with any method, there are both advantages and disadvantages. It is a useful technique in the development of a method that could be employed by a greater number of people given the resulting mathematical expression which is

indeed accomplished by Li et al. Also in a theoretical sense, Picard iteration can prove the existence of a solution and there is the possibility that it will guarantee convergence to a small interval depending on the formation of the right-hand side of the differential equation. But these advantages tend to be outweighed by the need for practicality in the context of real-world problems. [29: p.73]

However, there are also disadvantages in regards to this specific research topic. The approximated expression only solves for the net growth rate at each dilution level and is, therefore, restricted to that specific calculation. Nothing else can be determined from the equation, such as the phytoplankton biomass at each dilution, and it cannot be easily modified. For example, the approximation relies on the assumption that the zooplankton biomass is irrelevant, therefore, that parameter is not represented in the approximated equation making it impossible to test that assumption or modify the zooplankton growth rate. In addition, the Picard iteration method needs to be completed separately for each change in the functional response curve. This may lead to complications with the integration depending on the nature of the new response curve.

Therefore, similar to Charles Gallegos in 1989, the 4th order Runge-Kutta method with 5th order accuracy is the method employed in this research project. [30: p.145-146; 31: p.131]

$$K_1 = hf(t, x) \tag{5}$$
$$K_2 = hf(t + \frac{h}{2}, x + \frac{K_1}{2})$$
$$K_3 = hf(t + \frac{h}{2}, x + \frac{K_2}{2})$$
$$K_4 = hf(t + h, x + K_3)$$
$$x(t + h) = x(t) + \frac{1}{6}(K_1 + 2K_2 + 2K_3 + K_4)$$

Using the program available in Appendix A, the differential equation is solved using the estimated parameters from the Li et al. paper. However, the approximation equation has different parameters than the differential equation, specifically in regards to the grazing rate which can be seen in Table 3.

TABLE 3 – ORIGINAL DIFFERENTIAL EQUATION AND APPROXIMATION [9: P. 2-4]

Holling Type II	$\frac{dP}{dt} = \mu P - g_{max}\frac{P}{K+DP}DZ_0e^{vt}$
Li et al. Approximation	$\varepsilon_d = \mu - D\left(\frac{1+\frac{P_0}{K}}{1+D\frac{P_0}{K}}\right)\overline{m}$

As the approximation only estimates the mean grazing rate, a conversion is necessary to find the maximum grazing rate. This calculation comes from an intermediate equation for the approximation which is shown in Table 4.

TABLE 4 – FORMULAS FOR THE MEAN AND MAXIMUM GRAZING RATES [9: P. 2-4]

Holling Type II	$\overline{m} = \frac{g_{max}Z_0}{(K+P_0)}$	$g_{max} = \overline{m}\cdot\left(\frac{K+P_0}{Z_0}\right)$

Inputting the given and calculated parameters into the Runge-Kutta program, both the phytoplankton biomass and the net growth rate are calculated for each dilution rate while the approximation is also recreated for comparison purposes. Assessment of fit is determined by the sum of the squared error between the estimated values and the observed values taken from the estimated raw data in the Li et al. paper available in Appendix C.

Unlike Li et al., other functional response curves are considered in detail including the Holling Type I, Ivlev and hyperbolic tangent curves. The formulations of the resulting differential equations are available in Table 5 below. With each new equation, the corresponding maximum grazing rate is calculated from the formula for the mean grazing rate, the calculations of which can be found in Appendix B.

TABLE 5 – DIFFERENTIAL EQUATIONS WITH CORRESPONDING FUNCTIONAL RESPONSES

Holling Type I	$\frac{dP}{dt} = \mu P - g_{max} Z_0 e^{\nu t} \begin{cases} \frac{P}{2K} & , P_0 < 2K \\ 1 & , P_0 \geq 2K \end{cases}$
Ivlev	$\frac{dP}{dt} = \mu P - g_{max} \left(1 - e^{\frac{-P_0}{K}}\right) Z_0 e^{\nu t}$
Hyperbolic Tangent	$\frac{dP}{dt} = \mu P - g_{max} \tanh \frac{P_0}{K} Z_0 e^{\nu t}$

The corresponding computer codes are available in Appendix A.

3.3. Nonlinear Optimisation

Optimisation plays a critical role in fitting curves or models to available data by calculating the "minimisation (or the maximisation) of a function which depends on the solution of the model." [32: p.277] This is typically achieved by using the least squares technique which minimises the difference between the y values of the estimated and observed data points. This research requires two forms of optimisation, the first in finding the optimal parameter estimates for the phytoplankton growth rate, the half-saturation constant and the maximum grazing rate and the second in determining the best allocation of dilution rates.

3.3.1. Parameter Optimisation

Improving the model fit namely depends on adjusting the parameter estimates. This is achieved through optimisation which seeks to minimise the cost or objective function, in this case, the sum of the squared error or residuals between the observed and estimated values. [33: p.69] This equation takes the form:

$$sse = \sum_{i=1}^{N} (f(x_i) - y_i)^2 \quad (6)$$

In doing so, the approximated dilution rate data found in Appendix C are used as the x_i values. Through the Runge-Kutta method, the differential equation with specified functional response curve, or function f, is solved with the x_i dilution rates. The resulting net phytoplankton growth rates are differenced with the observed net growth rates, y_i, which are also approximated from the original Li et

al. paper. Each difference is squared before ultimately summing to achieve a goodness of fit measurement for the model which can then be used for comparison purposes.

The implementation of the procedure requires the MATLAB function *fminsearch* which performs an unconstrained optimisation employing the derivative-free Nelder-Mead simplex algorithm. [34] The Nelder-Mead algorithm is a direct-search method that begins with a simplex that "is the geometrical figure consisting, in N dimensions, of N + 1 points (or vertices) and all their interconnecting line segments, polygonal faces, etc." [35: p.408] The algorithm then conducts a series of steps, either a reflection, expansion, contraction or multiple contraction step, through the simplex moving from the highest point at the largest value down to the optimal point at the lowest function value. [35: p.408-409; 36: p.103]

In constructing the optimisation program, the *fminsearch* function requires the input of both the objective function to be minimised as well as an initial guess for parameters to be determined. To include variability, and determine the potential sensitivity, the initial guess is a vector of random values within a 15% interval, using the same method described in Section 3.1.2., above and below the given parameters. [27]

3.3.2. Standard Error and Confidence Intervals

After estimating the optimal values, standard errors and 95% confidence intervals are determined for each of the parameter estimates. The *fminsearch* function does not return either the standard error or confidence intervals for its estimates, therefore another function is used. The *nlinfit* MATLAB function is a nonlinear regression function that allows outputs of the parameter estimates, the residual vector and the Jacobian matrix. [37] The Jacobian matrix is the necessary component for the MATLAB function *nlparci* to calculate the confidence interval. [38] This function is only used when the parameter estimates match the estimates determined by *fminsearch,* otherwise the task is approached using Monte Carlo simulation. [39: p.104-106]

The *nlparci* function only returns the upper and lower bounds of the interval which requires the further calculation of the associated standard error using the equation:

$$CI = OpPar \pm t * SE \tag{7}$$

where CI is the confidence interval, $OpPar$ is the optimal parameter estimate, t is the t distribution statistic and SE is the standard error. [39: p.103]

3.3.3. Dilution Optimisation

On the other hand, the optimisation for the dilution rates necessitates a constrained approach using the MATLAB function *fmincon*. [40] In constrained optimisation, the constraints can take the form of inequalities or equalities in addition to upper and lower bounds. The nonlinear inequality and equality constraints must take the following form:

$$c(x) \leq 0 \tag{8}$$
$$ceq(x) = 0$$

which requires the rearrangement of some equations. There is also a choice in algorithm when using *fmincon*: the default interior-point, the SQP or SQP legacy, the active-set or the trust-region-reflective algorithm. For this project, the *fmincon* function relies on the default interior-point algorithm which "approaches constrained minimisation by solving a sequence of approximate minimisation problems." [41] The algorithm employs a barrier function and conducts either a direct or conjugate gradient step at each iteration with the direct option being the default option. [41]

For this optimisation, the cost function is the absolute value integral difference between the estimated functional response curve and the true functional response curve depicted as the shaded region in Figure 8. In constructing this cost function, the integration is calculated by the trapezoidal rule of integration using the MATLAB function *trapz* which calculates the numerical integration from discrete data inputs. [42] The process is applied to calculate the area beneath both curves before taking the absolute value difference between the two.

FIGURE 8 – DEPICTION OF THE DILUTION OPTIMISATION COST FUNCTION

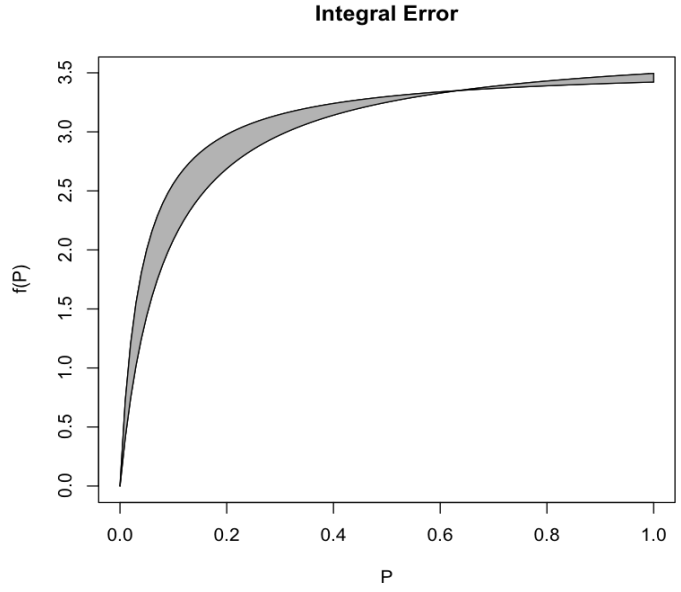

Similar to the parameter optimisation procedure, noise is added to each value of the initial guess vector at a level of 25%. The interval of dilution rates is also bounded at 0, for full dilution, and 1, for raw seawater. For the purposes of this task, six dilution rates, including a value at 1, are used meaning only five rates are the values to be optimised. In addition, there is a series of inequality constraints which takes the following form:

$$c(D) = \begin{bmatrix} D(1) - D(2) \\ D(2) - D(3) \\ D(3) - D(4) \\ D(4) - D(5) \end{bmatrix} \leq 0 \tag{9}$$

This set of nonlinear inequality constraints ensures that each successive dilution rate is greater than the last which maintains the order of dilutions from least to greatest.

3.3.4. New Method Development

The development of a new method regarding the identification of the functional response curve is attempted by utilising the information obtained in previous stages of this research project. Using the optimal parameters for the differential equation as the true functional response, the goal is to determine the optimal dilution rates that minimise the sum of the squared error and also converge to the true functional response. The procedure is as follows:

Step 1: Determine the parameter estimates for the 'true' functional response. For this project, the optimal parameters for the Holling II curve are used as the true response on which the error evaluation is based.

Step 2: Decide on two fixed dilution rates, one close to 0 and the other at 1. The first dilution rate for this task is fixed at 0.025.

FIGURE 9 – NEW METHOD INITIAL SIMULATION

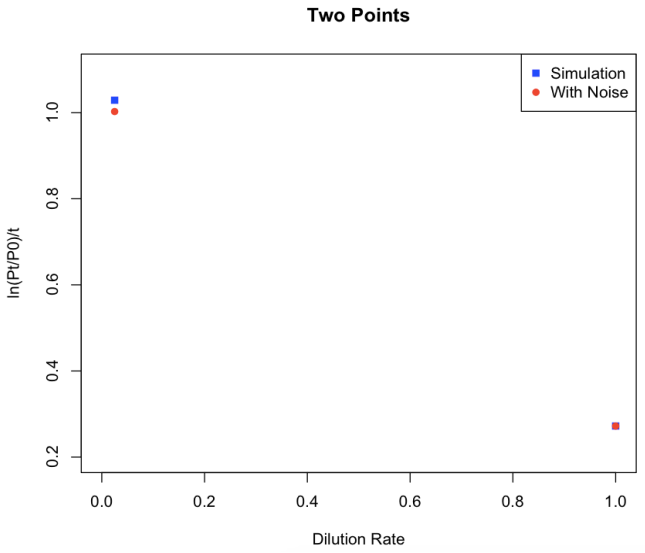

Step 3: Noise is added to the simulated data for the two fixed points as per the method described in Section 3.1.2. and shown in Figure 9. Those values are then saved for use in future steps.

FIGURE 10 – NEW METHOD INITIAL SIMULATION WITH OPTIMAL CURVE

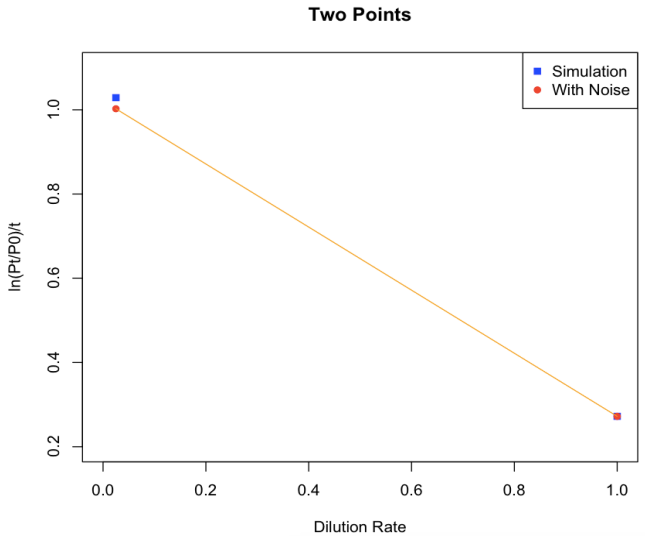

Step 4: The optimal parameters are then calculated to minimise the sum of the squared error between the noisy data points at the fixed dilution rates as depicted in Figure 10. The functional response curves are also plotted as seen in Figure 11.

FIGURE 11 – NEW METHOD INITIAL FUNCTIONAL RESPONSE

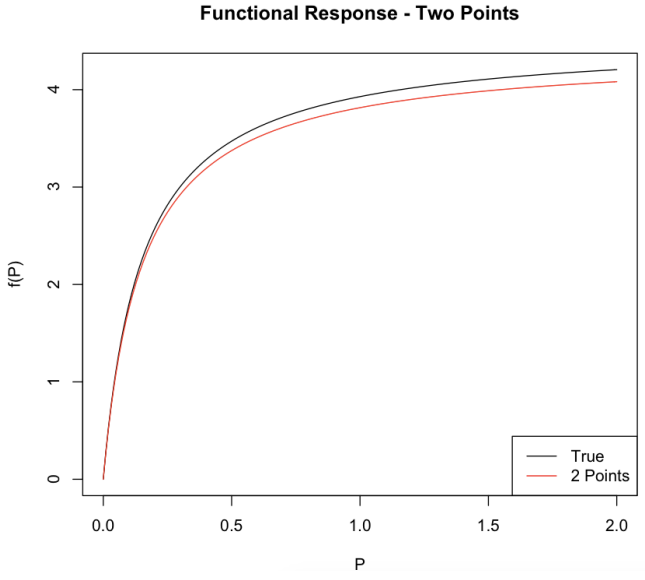

FIGURE 12 – EXAMPLE OF NEW METHOD WITH FIRST ADDITIONAL POINT

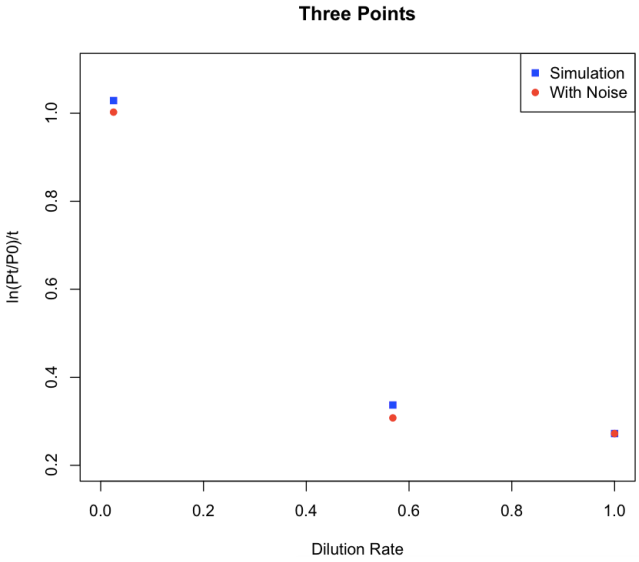

Step 5: The program then searches for an additional dilution rate and corresponding noisy data point (Figure 12) for which the optimal parameters will minimise the sum of the squared errors (Figure 13) as well as minimise the absolute value integral difference between the resulting functional response curve and the true response curve (Figure 14).

FIGURE 13 – OPTIMAL CURVE FOR 1ST ADDITIONAL POINT

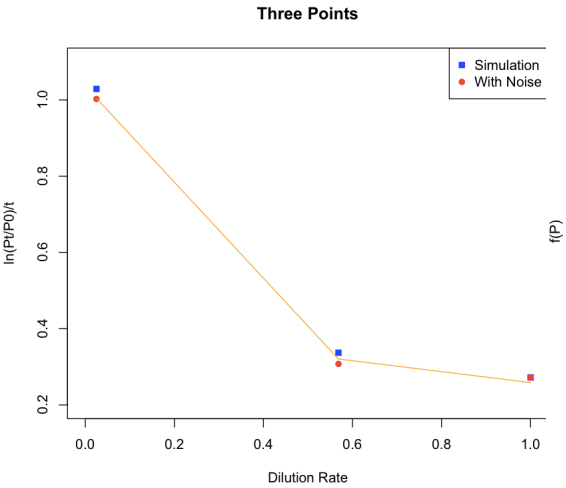

FIGURE 14 – FUNCTIONAL RESPONSE FOR 1ST ADDITIONAL POINT

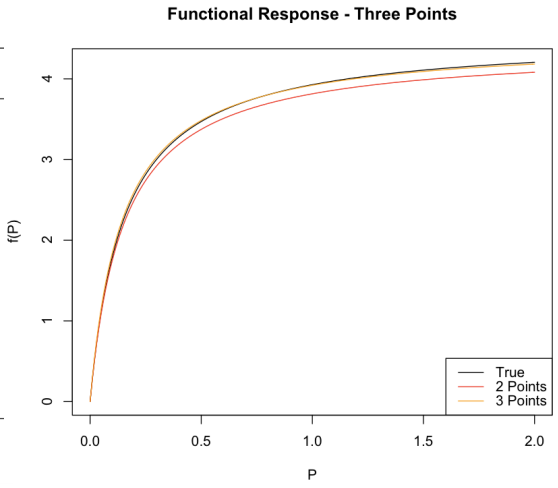

Step 6: All information is saved and all parameters are updated for use in the next iteration.

Step 7: Steps 1 through 6 are repeated until the desired number of dilution levels is reached. In the case of this research, the ultimate number of dilutions is six.

To accomplish this requires the changing of the parameter optimisation from an unconstrained to constrained approach. The constraints remain the same for the optimal dilution rate, with bounds at the two fixed points and the points remain in order. However, *fmincon* is now the function for the parameter optimisation with the inclusion of one inequality constraint. The objective function remains the minimisation of the sum of the squared error, but the constraint concerns the functional response.

As phytoplankton density, the half-saturation constant and the maximum grazing rate are the variables included in the various functional response curves, the optimal parameters are key to minimising the absolute integral difference. This is accomplished by constraining the difference to be less than the difference achieved at the previous point.

$$c(D) = D(n) + 0.05 - D(n-1) \leq 0 \qquad (10)$$

In addition, the nonlinear constraint equation (9) used in optimising a series of dilution rates no longer applies to this method and is replaced by a new constraint. As the first two dilution rates are fixed at 0.025 and 1, equation (10) ensures that the next additional point is less than, but not equal to, the previous rate of 1 with each subsequent dilution point decreasing towards the bound at 0.025. For this project and the total of six dilution rates, the value of 0.05 seemed reasonable to maintain distinct dilution rates, however, further experimentation could test the significance of this added value to the nonlinear constraint and its effect on the minimisation.

Chapter 4 – Results and Discussion

4.1. Finding the Optimal Parameters

4.1.1. Holling II

As the first consideration in this research project, the computational approach was compared to the approximation developed by Li et al. for the Holling II functional response curve. In comparing the two methods using the given estimated parameters, the approximation and differential equation are equally good, each having the minimum sum of squared error in two of the four cycles as seen in Table 6.

TABLE 6 – SUM OF SQUARED ERROR COMPARISON USING GIVEN PARAMETERS

Sum of Squares				
Cycle	**0601**	**0603**	**0604**	**0704**
Approximation	0.0462	0.1658	0.0462	0.1134
Differential Equation	0.0977	0.1717	0.0447	0.0976
Difference	-0.0515	-0.0059	0.0015	0.0158

However, as the differential equation had only been solved using estimated parameters, it was necessary to determine the parameters for which the curve best fits the available data. Using the approximated observed values available in Appendix C, the parameters μ, K, and g_{max} were optimised by minimising the sum of the squared error as described in the Methods section with the given estimated parameters used as the initial guess.

The resulting estimates for the phytoplankton growth rate, the half-saturation constant and the maximum grazing rate are shown in Table 7.

TABLE 7 – OPTIMAL PARAMETERS FOR THE HOLLING II DIFFERENTIAL EQUATION

Cycle	**0601**	**0603**	**0604**	**0704**
μ	1.3511	0.6506	0.7316	1.2067
K	0.1517	0.7529	0.9589	0.0388
g_{max}	4.5244	1.8518	4.3921	3.5547

Employing the optimal parameters in Table 7, the sum of squared error was calculated again with the observed data, the results of which are shown in Table 8.

TABLE 8 – SUM OF SQUARED ERROR COMPARISON USING OPTIMAL PARAMETERS

Optimal Parameters Sum of Squares				
Cycle	**0601**	**0603**	**0604**	**0704**
Approximation	0.0462	0.1658	0.0462	0.1134
Differential Equation	0.0449	0.1654	0.0442	0.0826
Difference	0.0013	0.0004	0.0020	0.0308

In comparing the findings in Table 8 to the original findings in Table 6, it is clear that the computational approach to solving the differential equation is more accurate than the Li et al. approximation. It is also interesting to note that, for cycles 0603 and 0604, the optimal parameters for the Holling II differential equation are similar to the approximation but they are vastly different for cycles 0601 and 0704 as shown in Table 9.

TABLE 9 – COMPARISON OF GIVEN (AP) AND OPTIMAL (DE) PARAMETER ESTIMATES

Cycle	**0601**		**0603**		**0604**		**0704**	
Method	**AP**	**DE**	**AP**	**DE**	**AP**	**DE**	**AP**	**DE**
μ	0.90	1.3511	0.64	0.6506	0.72	0.7316	0.92	1.2067
K	0.53	0.1517	0.84	0.7529	1.24	0.9589	0.20	0.0388
g_{max}	2.74	4.5244	1.76	1.8518	4.99	4.3921	3.25	3.5547

In fact, only three optimal parameters, the cycle 0601 half-saturation constant, the cycle 0603 phytoplankton growth rate and cycle 0603 half-saturation constant, fall within the confidence intervals of the corresponding given parameters. In addition, only the ratio between the initial phytoplankton biomass and the half-saturation constant for cycle 0603 is within the given confidence interval. The original data estimates with confidence intervals are available in Appendix C.

The discrepancies are more clear in Figures 15 through 18, where there are significant deviations in the curves for cycles 0601 and 0704, but very little for the other two cycles.

FIGURE 15 – DIFFERENTIAL EQUATION COMPARISON FOR CYCLE 0601

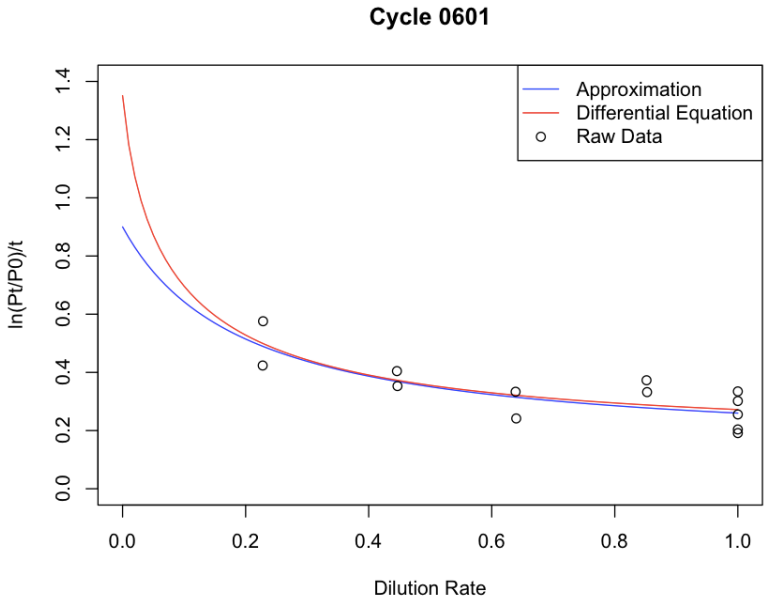

The optimal parameters for cycle 0601, shown in Figure 15, produced the most variation at the highest dilution levels compared to the blue approximation curve. However, moving from high to low dilution results in the red differential curve converging to the approximation at around the 0.2 dilution level with little divergence across the rest of the dilutions.

FIGURE 16 – DIFFERENTIAL EQUATION COMPARISON FOR CYCLE 0704

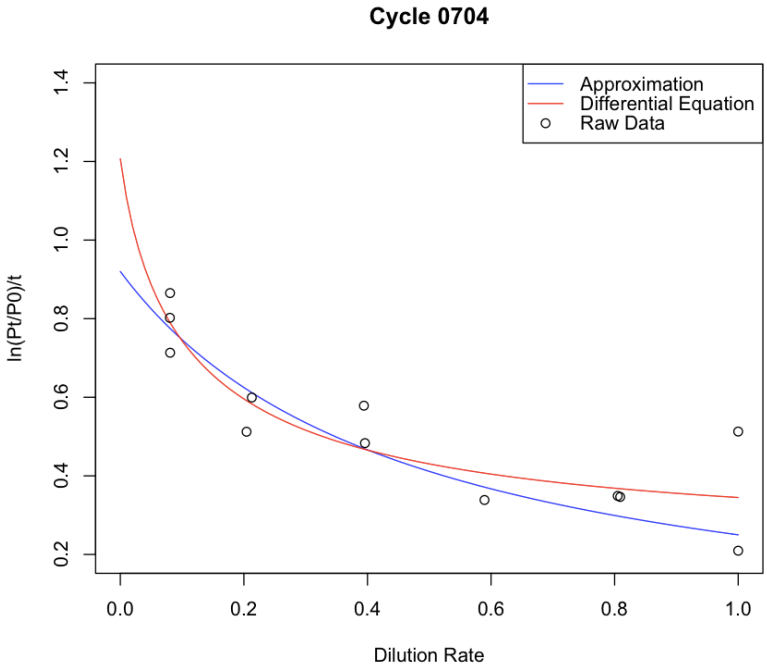

Unlike cycle 0601, cycle 0704 showed some level of variation over the entire range of dilutions as evidenced in Figure 16. The dissimilar shape of the cycle 0704 differential equation means that there is no convergence to the blue approximation curve as there is with cycle 0601 in Figure 15. The increased curvature also results in significant deviations at not only high dilution (near 0), but at raw seawater (near 1) levels as well.

FIGURE 17– DIFFERENTIAL EQUATION COMPARISON FOR CYCLE 0603

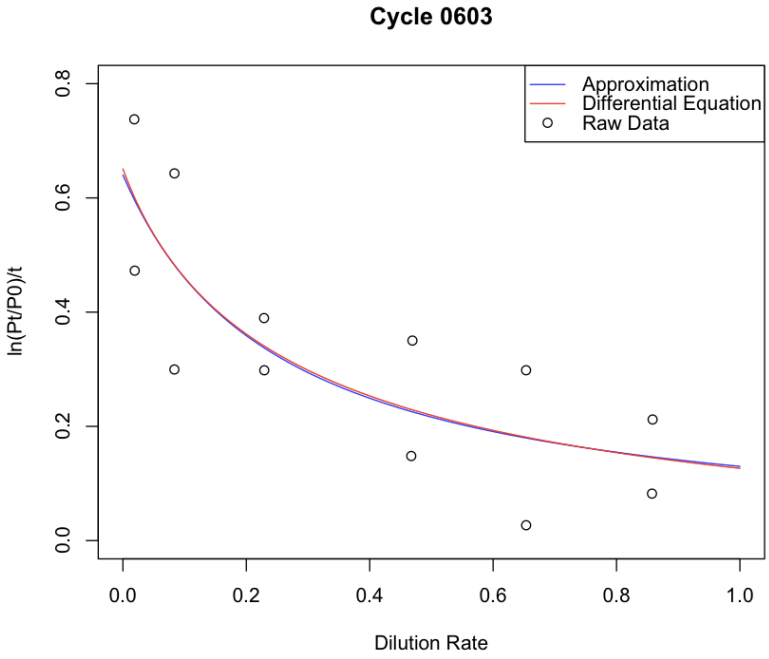

On the other hand, Figure 17 depicts the lack of significant deviations in net growth values or in the curvature of the two solutions for cycle 0603. In fact, the red differential curve can barely be distinguished from the blue approximation across the entire range of dilutions.

FIGURE 18 – DIFFERENTIAL EQUATION COMPARISON FOR CYCLE 0604

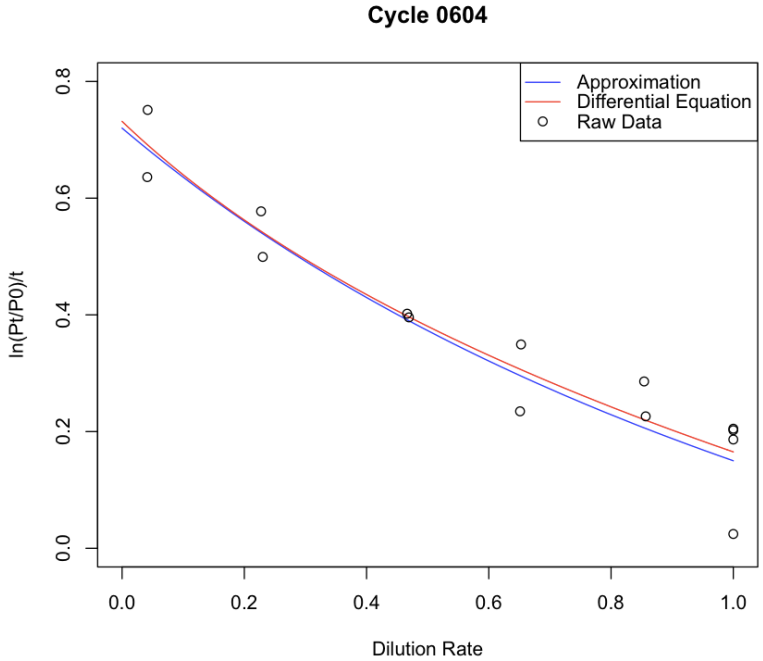

Though distinct curves, as visible in Figure 18, the results of cycle 0604 more closely resemble those of cycle 0603 than either of the other cycles. There is a very slight deviation at the highest dilution level as well as a somewhat consistent deviation towards lower dilutions but overall the curvature remains similar.

The variability in the optimal parameters is likely due to the lack of highly diluted samples for cycles 0601 and 0704. In the case of cycle 0601, there were no dilution points below the 0.2 level which presumably contributed to the large

disparity in the phytoplankton growth rate which is visible in the deviation at high dilution levels in Figure 15. The lack of divergence after the 0.2 level could potentially be due to the fact that the optimal half-saturation rate, though small, is still within the confidence interval of the given estimate. On the other hand, cycle 0704 included higher dilutions, at around 0.08, but it appears that level is still insufficient in determining an accurate phytoplankton growth rate. However, the significant difference in half-saturation estimates, including the confidence interval, may be a factor in the curvature variation in comparison to the approximation curve.

These results concerning the large disparity in phytoplankton growth rate estimates are in line with previous studies referenced in the literature review. As mentioned in Section 2.2., researchers such as Gallegos, Evans and Paranjape, Dolan, etc., for years, have recommended a dilution of at least 0.05 for the most accurate estimates of the phytoplankton intrinsic growth rate. The results of cycles 0603 and 0604 should be attributed to this recommendation as both cycles included dilution data at around 0.01 and 0.04 dilution levels, respectively.

Therefore, it appears that the Li et al. approximation using the Picard iteration method is quite accurate when high dilution data is present, but the differential equation is consistently the more accurate option.

4.1.2. Ivlev, Hyperbolic Tangent and Holling I

Moving on from the Holling II functional response curve, the procedure to determine the optimal parameters was completed again using the Ivlev, hyperbolic tangent and Holling I functional response curves. Referring to the calculations available in Appendix B, the necessary maximum grazing rate was determined for each of the additional responses. The calculated values, along with the given estimated phytoplankton growth rates and half-saturation constants, were used as the initial guesses for the, to be determined, optimal estimates. The resulting optimal parameters for each of the four cycles are included in the following tables, with the Holling II optimal parameters included for reference.

TABLE 10 – OPTIMAL PARAMETERS FOR ALL CYCLE 0601 FUNCTIONAL RESPONSES

Cycle 0601		Differential Optimal Parameters			
		Holling II	Ivlev	Tangent	Holling I
Given Parameters	P_0	2.6800	2.6800	2.6800	2.6800
	Z_0	0.7500	0.7500	0.7500	0.7500
Estimated Parameters	μ	1.3511	0.7757	0.7022	0.5214
	K	0.1517	0.8360	1.3347	2.1365
	g_{max}	4.5244	2.0884	1.7725	1.4986

TABLE 11 – OPTIMAL PARAMETERS FOR ALL CYCLE 0603 FUNCTIONAL RESPONSES

Cycle 0603		Differential Optimal Parameters			
		Holling II	Ivlev	Tangent	Holling I
Given Parameters	P_0	3.2900	3.2900	3.2900	3.2900
	Z_0	1.2000	1.2000	1.2000	1.2000
Estimated Parameters	μ	0.6506	0.6256	0.6070	0.5277
	K	0.7529	0.9027	1.2382	2.7634
	g_{max}	1.8518	1.4470	1.3504	2.3658

TABLE 12 – OPTIMAL PARAMETERS FOR ALL CYCLE 0604 FUNCTIONAL RESPONSES

Cycle 0604		Differential Optimal Parameters			
		Holling II	Ivlev	Tangent	Holling I
Given Parameters	P_0	0.6900	0.6900	0.6900	0.6900
	Z_0	0.2200	0.2200	0.2200	0.2200
Estimated Parameters	μ	0.7316	0.7275	0.7176	0.6761
	K	0.9589	0.6713	0.6804	0.6751
	g_{max}	4.3921	2.8429	2.3406	3.2449

TABLE 13 – OPTIMAL PARAMETERS FOR ALL CYCLE 0704 FUNCTIONAL RESPONSES

Cycle 0704		Differential Optimal Parameters			
		Holling II	Ivlev	Tangent	Holling I
Given Parameters	P_0	0.4300	0.4300	0.4300	0.4300
	Z_0	0.1300	0.1300	0.1300	0.1300
Estimated Parameters	μ	1.2067	0.9688	0.9106	0.7422
	K	0.0388	0.1081	0.1686	0.4383
	g_{max}	3.5547	2.4129	2.1726	3.0975

FIGURE 19 – OPTIMAL CURVES FOR CYCLE 0601

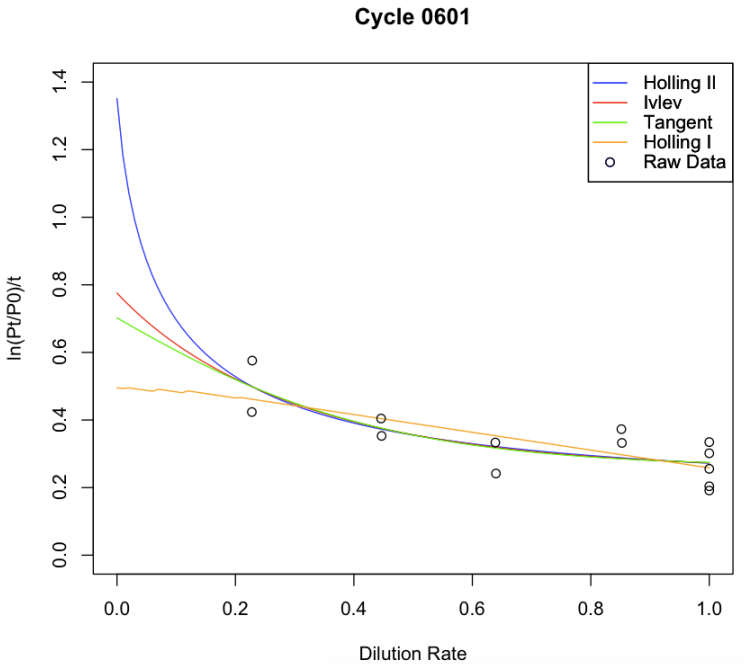

The Holling II, Ivlev and hyperbolic tangent curves for cycle 0601 had deviation at high dilution, especially for the blue Holling II curve, as evidenced in Figure 19. The three curves converge around the 0.2 dilution rate where they become indistinct from one another. The orange Holling I curve, on the other hand, has a lower y-intercept in comparison, though the linear response still appears to be a decent fit for the data after the 0.2 dilution level which is likely due to the smaller slope at lower dilution.

FIGURE 20 – OPTIMAL CURVES FOR CYCLE 0603

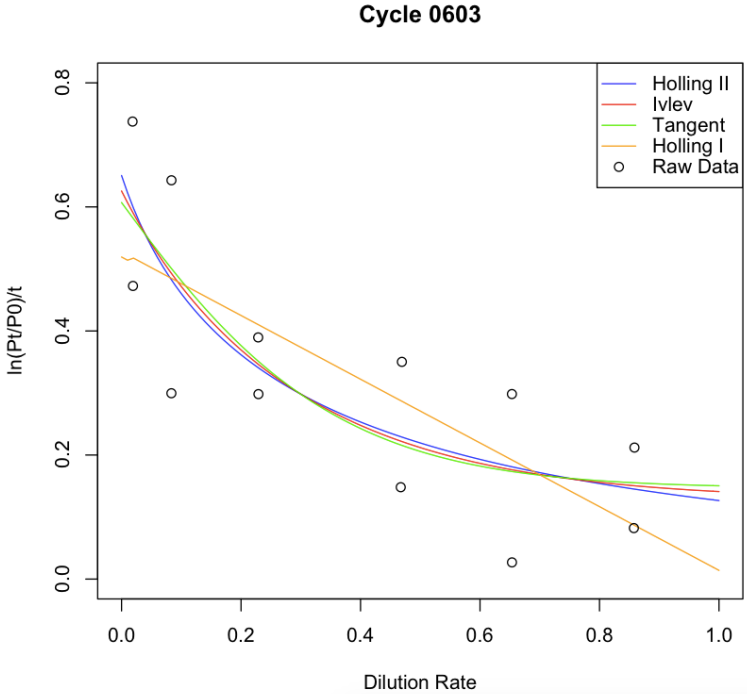

The Ivlev and hyperbolic tangent responses were very similar to the Holling II curve for cycle 0603, with very little deviation at both high and low dilution. The curves are close but still distinct which is clearly visible in Figure 20. In addition, the Holling I curve also seems to be a decent fit for the data and appears to minimise the absolute integral difference with the other three curves.

FIGURE 21 – OPTIMAL CURVES FOR CYCLE 0604

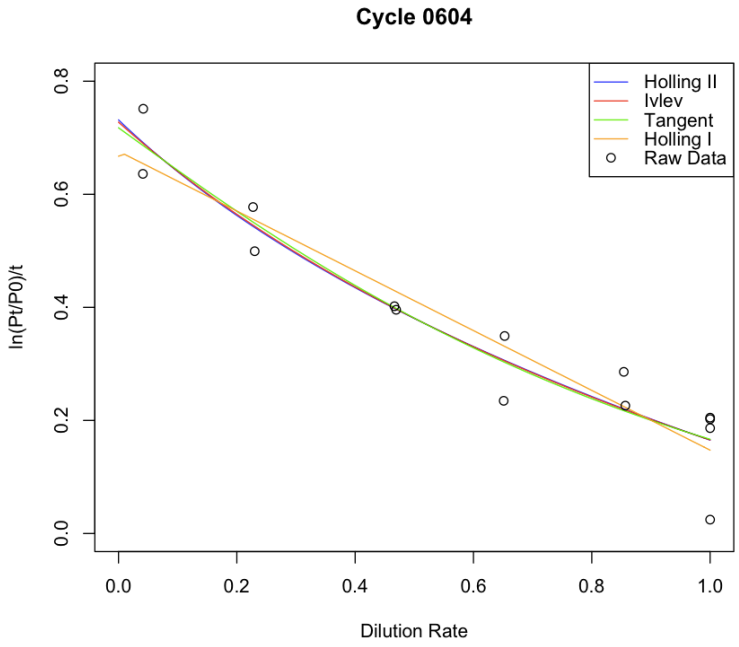

For cycle 0604, the Ivlev, hyperbolic tangent and Holling II curves in Figure 21 are indistinguishable from one another. Only the smallest deviation can be detected between the green hyperbolic tangent curve and the Ivlev and Holling II curves at the highest dilution level. The Holling I curve emphasises the lack of significant curvature present, appears to be a good fit for the data and, as with cycle 0603, it seems to minimise the integral difference between curves.

FIGURE 22 – OPTIMAL CURVES FOR CYCLE 0704

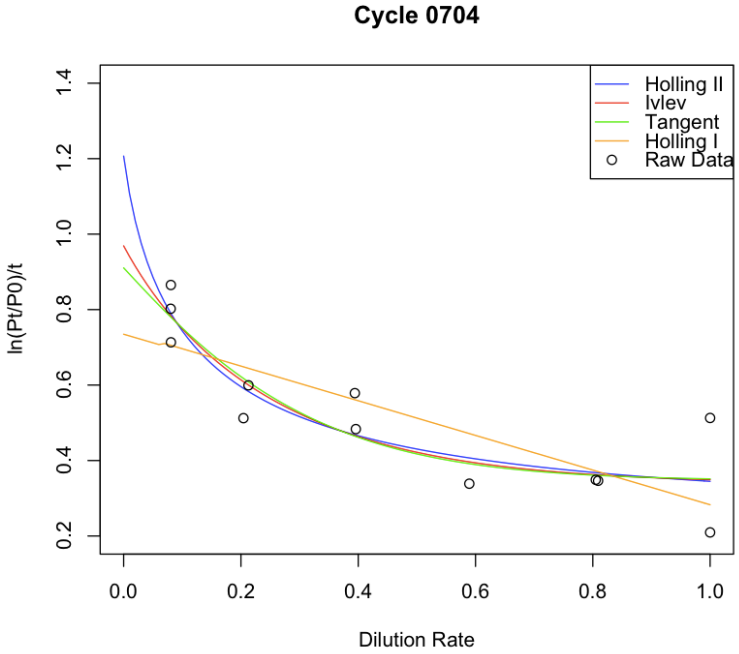

Similar to cycle 0601, cycle 0704 had deviations between the Holling II, Ivlev and hyperbolic tangent curves at high dilution levels. The three curves appear to converge around the 0.1 dilution rate, however, they don't remain as close as cycle 0601 for the duration of the dilution rates. In addition, while the Holling I curve has a greater deviation at the higher dilutions than low dilutions, it once again appears to minimise the integral difference between curves as seen in Figure 22.

TABLE 14 – SUM OF SQUARED ERROR FOR OPTIMAL FUNCTIONAL RESPONSES

Functional Response Sum of Squares				
Cycle	**Holling II**	**Ivlev**	**Tangent**	**Holling I**
0601	0.0449	0.0452	0.0454	0.0520
0603	0.1654	0.1669	0.1692	0.2002
0604	0.0442	0.0444	0.0450	0.0516
0704	0.0826	0.0843	0.0860	0.1389

In comparison to the Holling II curve, the corresponding sum of the squared error for each of the functional responses for all cycles is shown in Table 14. Each additional functional response has an increase in the sum of the squared error for all cycles.

In addition, while conducting this research, the parameter optimisation also revealed the potential significance of the ratio between the half-saturation constant and the maximum grazing rate. It was most apparent in the optimisation of the Holling I curve which was very sensitive to the initial parameter guess. During the optimisation process, the phytoplankton growth rates for some cycles remained consistent while the values for the half-saturation constant and maximum grazing rate varied widely. Further investigation revealed that some of the varying values retained the same ratio. It appeared that in these cases, the values were not necessarily optimal, instead, the specific combination of the half-saturation/maximum grazing ratio and the phytoplankton growth rate was optimal.

Considering this development, the same ratio was compared for the given and optimal parameters for the Holling II curve. Doing so revealed a significant outlier in the cycle 0601 ratio which was more than twice the next ratio in cycle 0603 as seen in Table 15 below.

TABLE 15 – GIVEN (AP) AND OPTIMAL (DE) HALF-SATURATION/MAXIMUM GRAZING RATIOS

Cycle	**0601**		**0603**		**0604**		**0704**	
Method	**AP**	**DE**	**AP**	**DE**	**AP**	**DE**	**AP**	**DE**
Ratio	0.193	0.034	0.477	0.407	0.249	0.218	0.062	0.011
Diff	0.159		0.070		0.031		0.051	

This is likely due to the difference of 1.7844 between the given and optimal maximum grazing parameter for cycle 0601, as shown in Table 9, which may once

again be attributed to the fact that cycle 0601 had no dilution data below 0.2 as with the other curves. Though cycle 0704, with its highest dilution at 0.08, may not have been sufficient in terms of the accuracy of the phytoplankton growth rate, it would seem that it was sufficient in specifically determining the maximum grazing rate. For reference, the difference between the given and optimal maximum grazing rate for cycle 0704 is 0.3047 which is almost one fifth the difference of cycle 0601.

The results of these ratios, as well as the variation in Tables 10 to 13, are more evident in the plotting of the four functional response curves for each of the four cycles where the x-axis represents the prey density and the y-axis represents the grazing response. Figure 23 illustrates the large difference for the Holling II maximum grazing rates especially for cycle 0601 and, to a lesser extent, cycle 0704.

FIGURE 23 – OPTIMAL FUNCTIONAL RESPONSE CURVES FOR CYCLES 0601 AND 0704

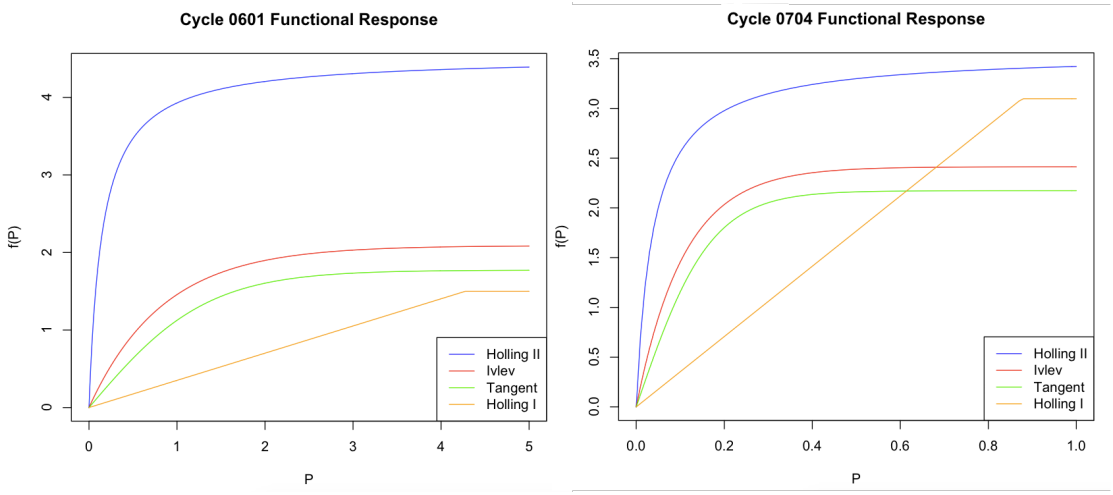

FIGURE 24 – OPTIMAL FUNCTIONAL RESPONSE CURVES FOR CYCLES 0603 AND 0604

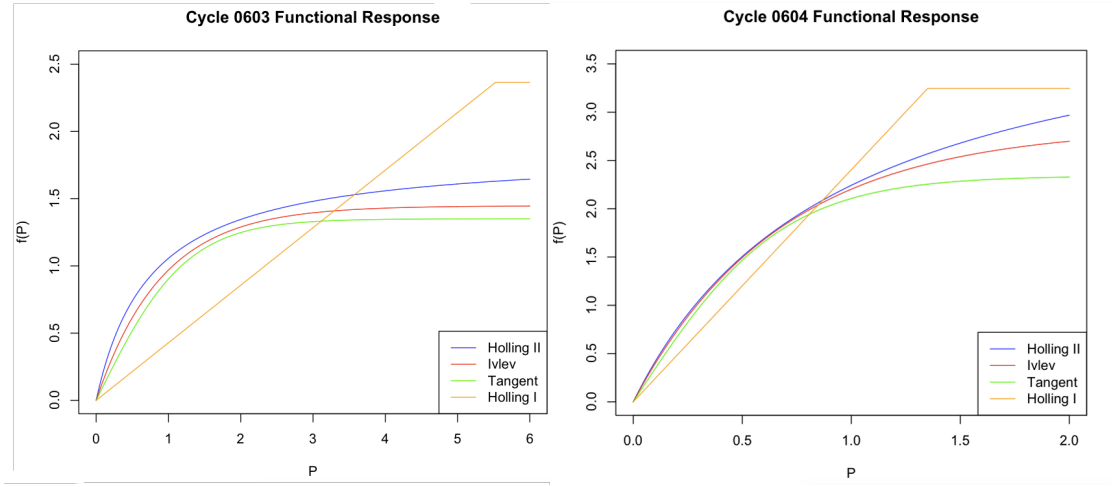

On the other hand, Figure 24 shows the lack of significant disparity between the maximum grazing rates of the Holling II, Ivlev and hyperbolic tangent responses for both cycles 0603 and 0604.

This research has confirmed that there are many factors to consider when choosing a functional response curve in the development of a plankton model and it is necessary to examine multiple options thoroughly to minimise the drawbacks and maintain accuracy.

4.1.3. Confidence Intervals

As parameter estimates are more useful when the standard error and confidence intervals are known, that was the next step for each of the three parameters, for all four cycles and all four functional response curves. As this is a great deal of data, only the information for cycle 0601 is included in Table 16.

TABLE 16 – STANDARD ERROR AND CONFIDENCE INTERVALS FOR CYCLE 0601

Cycle 0601				
Holling II	**Parameter Estimate**	**Standard Error**	**Confidence Interval**	
μ	1.3511	3.5259	-6.5050	9.2072
K	0.1517	1.0201	-2.1211	2.4246
g_{max}	4.5244	12.9461	-24.3212	33.3700
Ivlev	**Parameter Estimate**	**Standard Error**	**Confidence Interval**	
μ	0.7756	0.3029	0.1006	1.4506
K	0.8360	0.6993	-0.7221	2.3941
g_{max}	2.0884	1.0524	-0.2565	4.4334
Tangent	**Parameter Estimate**	**Standard Error**	**Confidence Interval**	
μ	0.7022	0.2096	0.2352	1.1692
K	1.3347	0.8179	-0.4879	3.1571
g_{max}	1.7725	0.7409	0.1217	3.4233
Holling I	**Parameter Estimate**	**Standard Error**	**Confidence Interval**	
μ	0.5214	4.5e-05	0.5213	0.5214
K	2.1365	6.7002	-4.5637	8.8367
g_{max}	1.4986	4.8148	-3.3162	6.3134

For cycle 0601, the Holling II optimal parameter estimates had the largest standard error and therefore, the largest confidence intervals of the four functional response curves. The standard errors significantly decreased for the Ivlev optimal parameters and both the phytoplankton growth rate and maximum grazing rates decreased again for hyperbolic tangent. The half-saturation standard error for the hyperbolic tangent curve was greater than Ivlev but still less than Holling II. The Holling I curve had the smallest standard error for the phytoplankton growth rate, the highest error for the half-saturation constant and only Holling II had a higher error for the maximum grazing rate. Similar results and patterns were found in the other three cycles, the data of which are available in Appendix C.

The fact that the Holling II functional response has the lowest sum of the squared error, but also the highest parameter standard error, reiterates the need for testing additional models as what appears to be the best fit at first may have unforeseen drawbacks.

4.2. Determining a Set of Optimal Dilution Rates

The first analysis relating to dilution levels consists of comparing the different allocations of six dilution rates for the Holling II curve. In consideration are four combinations as listed in Table 17: a uniform distribution (Distribution 1), one with a cluster in the middle (Distribution 2), one with a cluster towards low dilution (Distribution 3), and another with a cluster towards high dilution (Distribution 4). In doing so, insight is derived concerning the likelihood of the optimal allocation of dilution rates. The comparison is assessed by both the sum of the squared error and the absolute integral error which are listed in Table 18.

TABLE 17 – DILUTION RATE DISTRIBUTIONS

Distribution 1-uniform	0.1665	0.3330	0.4995	0.6660	0.8325	1.0000
Distribution 2-middle	0.1000	0.3000	0.3500	0.4000	0.4500	1.0000
Distribution 3-low	0.1000	0.2000	0.5000	0.8000	0.9000	1.0000
Distribution 4-high	0.0500	0.0750	0.1000	0.2000	0.5000	1.0000

In conducting this segment of the project, simulated data was randomly chosen at a 25% noise level for the given dilution distribution before the optimal

parameters were found and the sum of the squared error, as well as the absolute integral error, were calculated. The optimal parameters listed in Table 7 were used as the true functional response for comparison purposes. This process was repeated 50 times before being averaged to find the resulting estimates and errors. The focus was not necessarily on the estimated parameters, but on the error values.

TABLE 18 – SUM OF SQUARED (SSE) AND ABSOLUTE INTEGRAL ERRORS (FRC) FOR TABLE 17

Cycle	0601		0603		0604		0704	
Err	SSE	FRC	SSE	FRC	SSE	FRC	SSE	FRC
1	0.0018	14.458	6.7e-4	3.928	0.0018	0.551	0.0032	24.243
2	0.0026	6.806	0.0011	0.517	0.0037	0.304	0.0034	10.231
3	0.0015	20.375	7.0e-4	2.287	0.0021	0.448	0.0028	9.205
4	0.0060	5.098	0.0026	0.371	0.0046	0.210	0.0085	1.397

The sum of the squared error was less than or equal to 0.0085 for each of the cycles at the various dilution distributions which is less than all the sums of the squared error found in Section 4.1. On the other hand, the integral error ranged from a minimum of 0.21 for cycle 0604, Distribution 4, to a maximum of 20.375 for cycle 0601, Distribution 3.

The best distribution by far, with minimum integral error for all four cycles, is Distribution 4 which has four dilution rates less than or equal to 0.2. For three out of four cycles, cycles 0603, 0604, and 0704, the uniform distribution (Distribution 1) is the worst allocation of points in terms of accuracy in regards to the true functional response curve. Cycles 0601, 0603 and 0604, provide evidence that an allocation of points with a cluster around the middle dilution levels, or a distribution with 5 out of 6 dilution rates below 0.5 dilution, is a better option than both the uniform distribution and the allocation with a cluster towards low dilution. This leads to the conclusion that 5 out of 6 dilution rates should be equal to or less than 0.5, but better results will occur if more of those points fall equal to or below 0.2 dilution. This is consistent with previous results found by Gallegos, Evans and Paranjape, Dolan, Chen, etc.

This insight was further tested by optimising a vector of dilution points using the constrained optimisation method described in Section 3.3.3. The vector included six dilution points, though only five were optimised as the sixth was fixed

at 1. In conducting this test, two versions of the program were used: one version containing optimal parameters determined through unconstrained optimisation and the other through constrained optimisation as described in Section 3.3.4. The four distributions listed in Table 19 were used as the initial guesses in determining the optimal dilution rates with 25% added noise. The results of both versions of the approach are shown in Tables 19 to 22.

TABLE 19 – OPTIMAL DILUTION RATES FOR UNIFORM DILUTION INITIAL GUESS

Distribution 1								
Initial Guess	Unconstrained Parameters				Constrained Parameters			
	0601	0603	0604	0704	0601	0603	0604	0704
0.1665	0.709	0.1519	0.1765	0.0016	0.1361	0.1909	0.1707	0.3888
0.3330	0.710	0.3194	0.2838	0.3588	0.3048	0.3522	0.3351	0.5051
0.4995	0.710	0.4774	0.4909	0.4213	0.4664	0.5563	0.5039	0.6832
0.6660	0.793	0.5999	0.6502	0.6867	0.6406	0.7287	0.7024	0.7672
0.8325	0.913	0.8213	0.8125	0.8813	0.8163	0.8038	0.9565	0.8990
1.0000	1.000	1.0000	1.0000	1.0000	1.0000	1.0000	1.0000	1.0000

TABLE 20 – OPTIMAL DILUTION RATES FOR MIDDLE DILUTION CLUSTER INITIAL GUESS

Distribution 2								
Initial Guess	Unconstrained Parameters				Constrained Parameters			
	0601	0603	0604	0704	0601	0603	0604	0704
0.10	0.0754	0.0003	0.3351	0.2987	0.1171	0.1087	0.0859	0.0904
0.30	0.2587	0.2005	0.3351	0.3783	0.3002	0.3044	0.3276	0.2877
0.35	0.4251	0.2888	0.4202	0.4135	0.4563	0.3478	0.3317	0.3161
0.40	0.5114	0.3607	0.5044	0.4596	0.5664	0.3901	0.3704	0.3727
0.45	0.5150	0.4405	0.6910	0.6012	0.6568	0.4022	0.3712	0.4232
1.00	1.0000	1.0000	1.0000	1.0000	1.0000	1.0000	1.0000	1.0000

TABLE 21 – OPTIMAL DILUTION RATES FOR LOW DILUTION CLUSTER INITIAL GUESS

Distribution 3								
Initial Guess	Unconstrained Parameters				Constrained Parameters			
	0601	0603	0604	0704	0601	0603	0604	0704
0.1	0.1157	0.0510	0.0679	0.0963	0.0658	0.1009	0.1044	0.0824
0.2	0.2018	0.1469	0.1399	0.2253	0.1318	0.2085	0.1961	0.1751
0.5	0.4818	0.5557	0.6476	0.4079	0.3536	0.5176	0.5212	0.4778
0.8	0.7871	0.8147	0.8512	0.8824	0.6338	0.6954	0.7868	0.7375
0.9	0.8266	0.9255	0.8760	0.8888	0.8836	0.7989	0.9188	0.8931
1.0	1.0000	1.0000	1.0000	1.0000	1.0000	1.0000	1.0000	1.0000

TABLE 22 – OPTIMAL DILUTION RATES FOR HIGH DILUTION CLUSTER INITIAL GUESS

Distribution 4								
Initial	Unconstrained Parameters				Constrained Parameters			
Guess	0601	0603	0604	0704	0601	0603	0604	0704
0.050	0.0314	0.0501	0.0419	0.0938	0.0442	0.0537	0.1224	0.1106
0.075	0.0469	0.0788	0.0701	0.1536	0.0749	0.0879	0.1412	0.1197
0.100	0.0568	0.1157	0.0981	0.1718	0.0919	0.0924	0.1841	0.1327
0.200	0.1214	0.2061	0.1957	0.1938	0.1960	0.2049	0.2134	0.1997
0.500	0.5644	0.5052	0.5449	0.4697	0.4929	0.5503	0.5013	0.4958
1.000	1.0000	1.0000	1.0000	1.0000	1.0000	1.0000	1.0000	1.0000

Given the previous results, the assumption was that Distribution 4, with multiple high dilution points, would achieve the minimal error, however, that was not the case. The resulting optimal allocations of points using both unconstrained and constrained parameters appear to be sensitive to the initial guess vector. This is especially visible in the constrained cycle 0603 in Table 20, the constrained cycle 0604 in Table 21, and the constrained cycle 0601 as well as the unconstrained cycle 0603 in Table 22.

In terms of assessment, Table 23 lists the sum of the squared error for each cycle, both constrained and unconstrained, for each initial distribution guess. Overall, the unconstrained parameters resulted in the lower sum of the squared error for all but four of the cycles: cycle 0603 for Distribution 2, cycle 0601 for Distribution 3 and cycles 0603 and 0604 for Distribution 4. For those four cycles, the constrained parameter version produced the minimum sum of the squared error.

TABLE 23 – SUM OF SQUARED ERROR FOR THE OPTIMAL DILUTION RATES

	Unconstrained Parameters				Constrained Parameters			
Dist	0601	0603	0604	0704	0601	0603	0604	0704
1	2.7e-3	6.3e-4	9.1e-4	1.8e-3	5.9e-3	7.8e-4	6.0e-3	3.0e-3
2	3.9e-4	8.6e-4	6.9e-4	3.6e-4	1.8e-3	1.8e-5	2.9e-3	5.7e-3
3	3.4e-3	5.9e-4	8.7e-4	1.9e-3	4.2e-4	1.1e-3	3.0e-3	5.7e-3
4	5.7e-4	1.8e-3	1.5e-2	6.7e-3	3.38e-2	1.6e-3	4.1e-3	1.61e-2

More importantly, though, is the assessment with regards to the absolute integral difference between the functional response curves. The integral errors are listed in Table 24 and show equal but opposite results compared to the sum of the squared error in Table 23. In this case, the constrained parameters produced

the lower absolute integral error in all but four cycles: cycle 0603 for Distributions 1, 2 and 4 as well as cycle 0704 for Distribution 1. For those four cycles, the unconstrained parameters minimised the error more effectively. Therefore, as the goal for the optimal allocation of dilution rates is to minimise the absolute integral difference between the functional response curves, it is necessary to constrain the parameter optimisation as well as the dilution optimisation.

TABLE 24 – ABSOLUTE INTEGRAL ERROR FOR THE OPTIMAL DILUTION RATES

	Unconstrained Parameters				Constrained Parameters			
	0601	0603	0604	0704	0601	0603	0604	0704
Dist 1	5.114	1.510	0.196	0.066	1.0e-4	5.332	8.9e-5	0.666
Dist 2	7.513	0.111	0.680	2.826	2.1e-4	0.734	0.261	1.326
Dist 3	2.360	0.131	0.067	1.598	3.4e-4	0.002	7.2e-6	2.6e-4
Dist 4	1.769	0.215	0.301	2.998	3.6e-4	0.721	7.3e-6	0.666

In terms of the unconstrained optimal parameters, no distribution was dominant and each cycle produced the minimum integral error given a different initial distribution guess vector. Though the results were different for each of the four cycles, the first dilution point was below 0.07 for all four cycles as seen in Table 25.

TABLE 25 – OPTIMAL DILUTION RATE ALLOCATION FOR EACH CYCLE

Unconstrained Parameters				Constrained Parameters			
0601	0603	0604	0704	0601	0603	0604	0704
Dist 4	Dist 2	Dist 3	Dist 1	Dist 1	Dist 3	Dist 3	Dist 3
0.0314	0.0003	0.0679	0.0016	0.1361	0.1009	0.1044	0.0824
0.0469	0.2005	0.1399	0.3588	0.3048	0.2085	0.1961	0.1751
0.0568	0.2888	0.6476	0.4213	0.4664	0.5176	0.5212	0.4778
0.1214	0.3607	0.8512	0.6867	0.6406	0.6954	0.7868	0.7375
0.5644	0.4405	0.8760	0.8813	0.8163	0.7989	0.9188	0.8931
1.0000	1.0000	1.0000	1.0000	1.0000	1.0000	1.0000	1.0000

However, for the constrained optimal parameters, Distribution 3, which skewed towards low dilution, was the dominant initial guess for determining the minimal functional response error for cycles 0603, 0604 and 0704. Even so, the first dilution point was below 0.14 for all four cycles with constrained parameters. In fact, for cycles 0603, 0604 and 0704, the first two dilution rates fall equal to or below 0.2085.

These results are likely due to sensitivity regarding the initial guess distributions and therefore, may not be entirely accurate due to lack of sufficient time to complete multiple simulations. More insight could be derived about the sensitivity if Monte Carlo simulation was completed and the results averaged.

4.3. Testing the New Method

For the purposes of this experiment, the optimal parameters determined in Section 4.1. for the Holling II curve were considered to be the true response in order to judge effectiveness. In experimenting with and developing the new method, the first two dilution rates were fixed at 0.025 and 1. These rates were used in a simulation program to find the first two data points within a noise interval of 25% above and below simulated data point as previously described in the Methods section. The true optimal parameters were also fixed as the parameters for the simulation program to maintain consistency. The resulting data points were saved and subsequently used as the estimated values in determining the optimal parameters.

The final dilution rates, as well as the optimal parameters, for all four cycles, are available in Tables 26 to 29. In addition, the simulated data and data points with noise are also included for reference.

TABLE 26 – NEW METHOD RESULTS FOR CYCLE 0601

Cycle 0601						
Parameter	True	2 Points	3 Points	4 Points	5 Points	6 Points
μ	1.3511	1.3184	1.3362	1.3403	1.3438	1.3354
K	0.1517	0.1503	0.1433	0.1392	0.1689	0.1273
g_{max}	4.5244	4.3885	4.4833	4.4632	4.6075	4.4037
Dilution	0.0250	1.0000	0.5685	0.1501	0.0639	0.0250
+ Noise	1.0025	0.2721	0.3077	0.6037	0.7862	0.9474
Simulation	1.0288	0.2722	0.3370	0.5953	0.8106	1.0288

TABLE 27 – NEW METHOD RESULTS FOR CYCLE 0603

Cycle 0603						
Parameter	True	2 Points	3 Points	4 Points	5 Points	6 Points
μ	0.6506	0.6256	0.6363	0.6267	0.6274	0.6515
K	0.7529	0.8001	0.8628	0.7545	0.7541	0.6793
g_{max}	1.8518	1.7658	1.8254	1.7448	1.7475	1.8013
Dilution	0.0250	1.0000	0.2700	0.2264	0.1140	0.0358

+ Noise	0.5674	0.1326	0.3393	0.3080	0.4322	0.5802
Simulation	0.5863	0.1266	0.3148	0.3424	0.4430	0.5632

TABLE 28 – NEW METHOD RESULTS FOR CYCLE 0604

Cycle 0604						
Parameter	True	2 Points	3 Points	4 Points	5 Points	6 Points
μ	0.7316	0.7121	0.7205	0.7204	0.7354	0.7465
K	0.9589	1.1225	0.8132	1.0600	1.0383	0.9929
g_{max}	4.3921	4.6154	3.9673	4.5390	4.5625	4.4651
Dilution	0.0250	1.0000	0.2669	0.1711	0.1211	0.0531
+ Noise	0.6899	0.1695	0.4934	0.6089	0.6738	0.6813
Simulation	0.7070	0.1652	0.5170	0.5838	0.6227	0.6808

TABLE 29 – NEW METHOD RESULTS FOR CYCLE 0704

Cycle 704						
Parameter	True	2 Points	3 Points	4 Points	5 Points	6 Points
μ	1.2067	1.2552	1.1749	1.2098	1.1374	1.2006
K	0.0388	0.0404	0.0739	0.0374	0.0811	0.0433
g_{max}	3.5547	3.8010	3.7004	3.5469	3.7783	3.5804
Dilution	0.0250	1.0000	0.5125	0.1631	0.0858	0.0294
+ Noise	1.0448	0.3300	0.4577	0.5882	0.7584	1.0295
Simulation	1.0031	0.3449	0.4268	0.6383	0.7764	0.8786

While it is clear that the method needs additional work and improvement, it currently produces results consistent with previous findings in this section as well as other studies. The contrast to the results of the optimal dilution allocation in the previous task can likely be attributed to the lack of specific fixed initial guesses required for this method as opposed to either version of the previous program. With the new method requiring an initial guess of the mean of the current dilution points, there appears to be no influence or sensitivity in the determination of the additional points.

The method is meant to continually minimise the error between the functional response curves with each additional dilution point until it eventually converges to the true functional response. The method currently accomplishes that goal to a certain extent, much of the time, as evidenced in Table 30 where the minimal error occurs at 5 points for 3 out of the 4 cycles. However, while the addition of the 6th point increases the error, it is not a substantial amount with the greatest increase being 1.71e-04.

TABLE 30 – NEW METHOD ABSOLUTE INTEGRAL ERROR FOR ALL CYCLES

Functional Response Error					
Cycle	2 Points	3 Points	4 Points	5 Points	6 Points
0601	0.206511	1.17e-04	3.59e-04	3.92e-06	1.80e-04
0603	0.134221	0.134179	0.111144	0.107984	0.027459
0604	0.108177	0.108098	0.061365	8.53e-05	1.14e-04
0704	0.436711	0.073695	4.61e-04	3.46e-04	3.63e-04

These results are more visible in the following figures depicting the functional response curves at both five and six points for all four cycles. The green curve representing the results of six points is clearly an improvement in the case of cycle 0603 as seen in Figure 26, but the difference is hard to see for the other three cycles.

FIGURE 25 – CYCLE 0601 FUNCTIONAL RESPONSE CURVES UP TO FIVE AND SIX POINTS

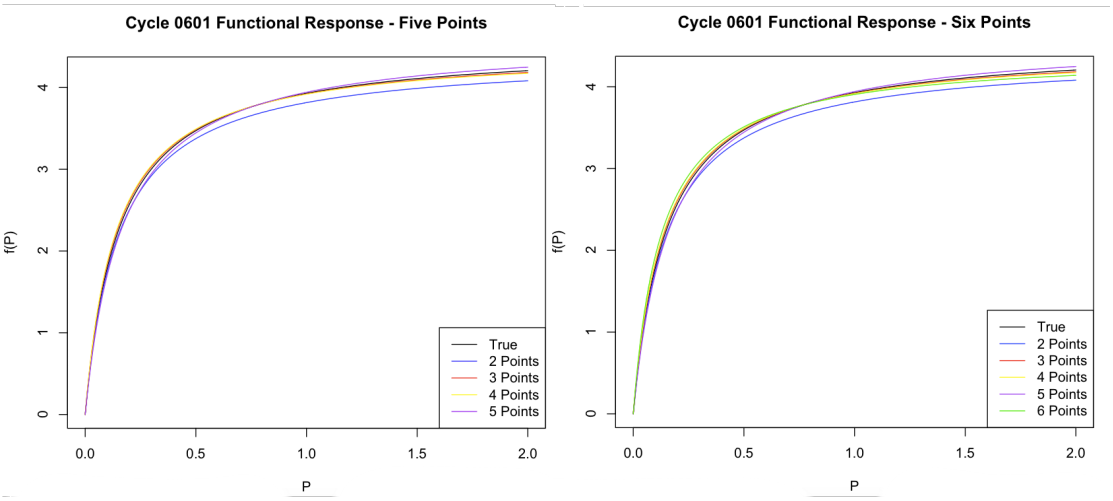

FIGURE 26 – CYCLE 0603 FUNCTIONAL RESPONSE CURVES UP TO FIVE AND SIX POINTS

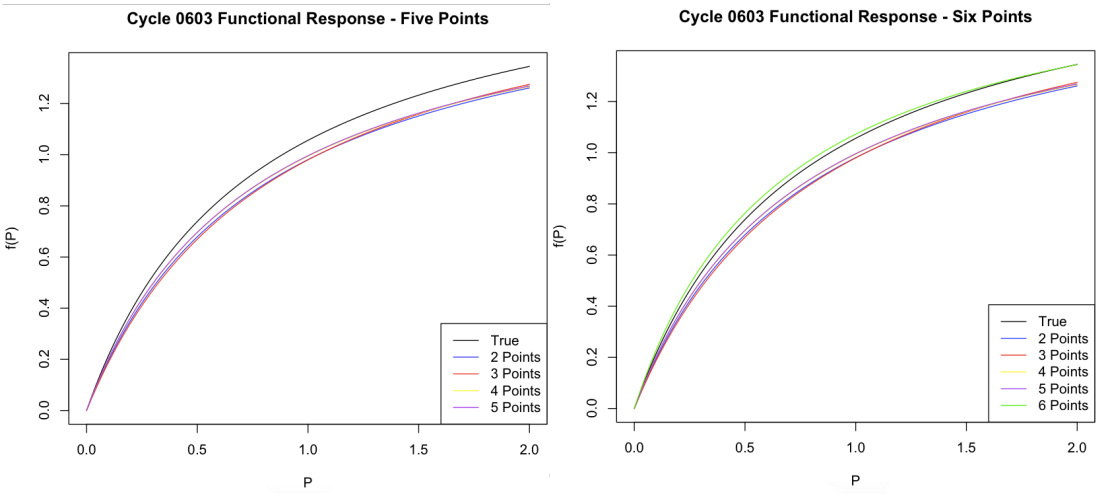

FIGURE 27 – CYCLE 0604 FUNCTIONAL RESPONSE CURVES UP TO FIVE AND SIX POINTS

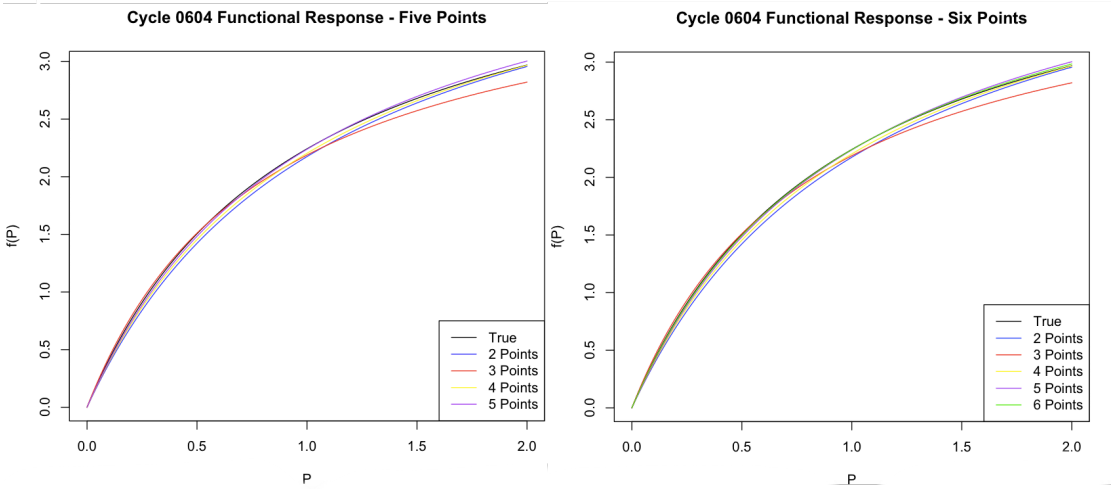

FIGURE 28 – CYCLE 0704 FUNCTIONAL RESPONSE CURVES UP TO FIVE AND SIX POINTS

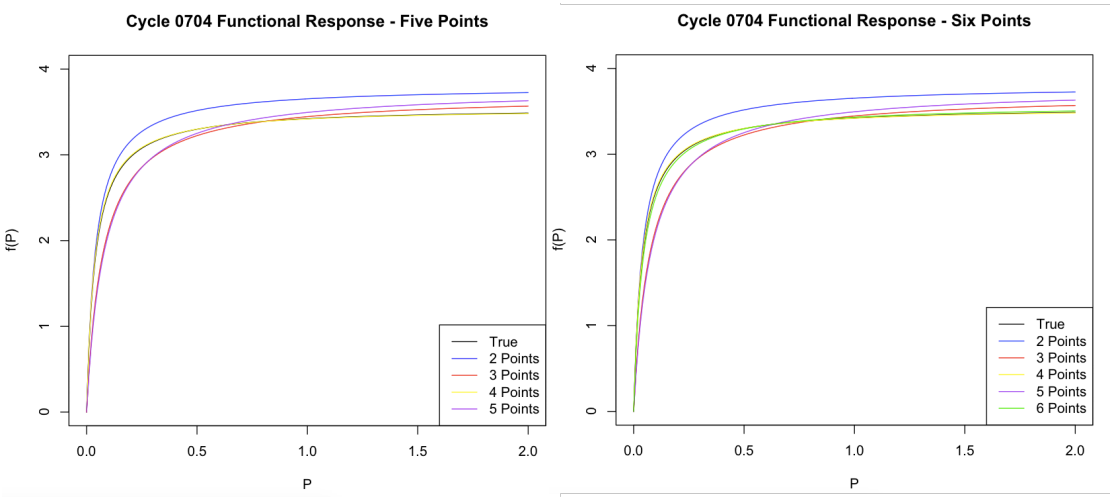

The final dilution rates are shown, in order, in Table 31 which clearly shows a similarity between cycles 0601 and 0704 as well as between cycles 0603 and 0604. This is consistent with previous findings describing greater deviations between the differential equations for cycles 0601 and 0704 and the approximations which have been attributed to the lack of high dilution data points. As there was more curvature for the 0601 and 0704 optimal curves, the inclusion of a point at around half dilution makes sense as the goal is to detect the nonlinear aspects of the curves.

TABLE 31 – ORDERED OPTIMAL DILUTION ALLOCATION FOR ALL CYCLES

Cycle 0601	Cycle 0603	Cycle 0604	Cycle 0704
0.0250	0.0250	0.0250	0.0250
0.0250	0.0358	0.0531	0.0294
0.0639	0.1140	0.1211	0.0858
0.1501	0.2264	0.1711	0.1631
0.5685	0.2700	0.2669	0.5125
1.0000	1.0000	1.0000	1.0000

On the other hand, the differential equations for cycles 0603 and 0604 were much closer to the approximations and other functional response curves and, therefore, require a different allocation of points. For these two cycles, 5 of the points are equal to or less than 0.27 with both having an additional point below 0.1 dilution. The only difference between the two results is that cycle 0603 has two points within 0.2-0.3 dilution range while cycle 0604 has two points between 0.1-0.2 range. This is likely indicative of the more linear nature of the cycle 0604 curve which would not necessitate a wide distribution of dilution points.

Looking further into the allocation, specifically at the point where the error is minimal at 5 points results in Table 32 below which simply removes an additional point that falls below the 0.1 dilution level.

TABLE 32 – ORDERED OPTIMAL DILUTION ALLOCATION TERMINATING AT MINIMAL ERROR

Cycle 0601	Cycle 0604	Cycle 0704
0.0250	0.0250	0.0250
0.0639	0.1211	0.0858
0.1501	0.1711	0.1631
0.5685	0.2669	0.5125
1.0000	1.0000	1.0000

The difference that results in terminating at the fifth point, which is especially clear for cycles 0601 and 0704, is illustrated in Figures 29 to 31. The lack of an additional point at high dilution removes the added noise which, in such close proximity to the initial fixed point and the proportionally large noise interval, likely caused the nominal increase in the absolute integral difference at six dilution points.

FIGURE 29 – CYCLE 0601 NEW METHOD DILUTION PLOT FOR FIVE AND SIX POINTS

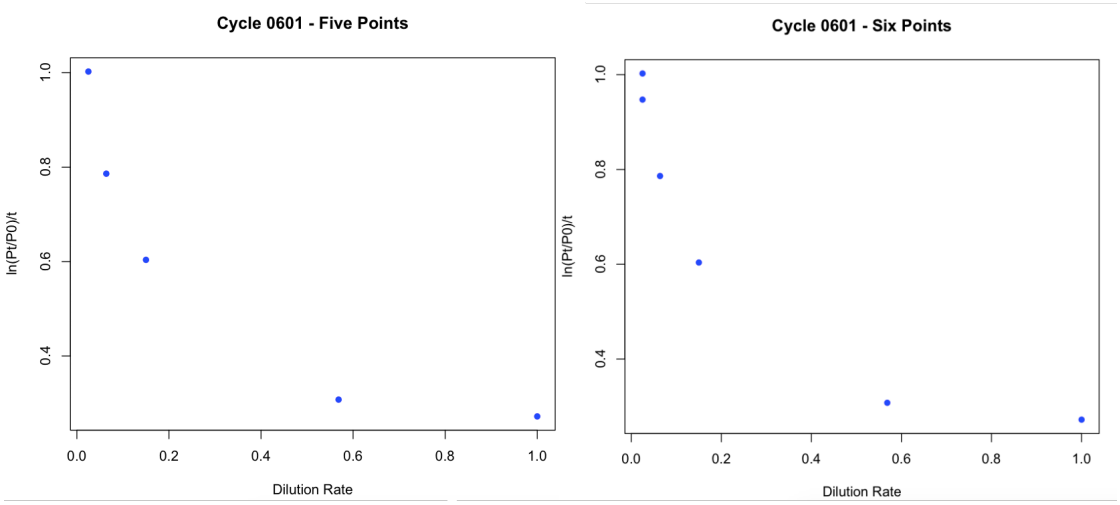

FIGURE 30 – CYCLE 0604 NEW METHOD DILUTION PLOT FOR FIVE AND SIX POINTS

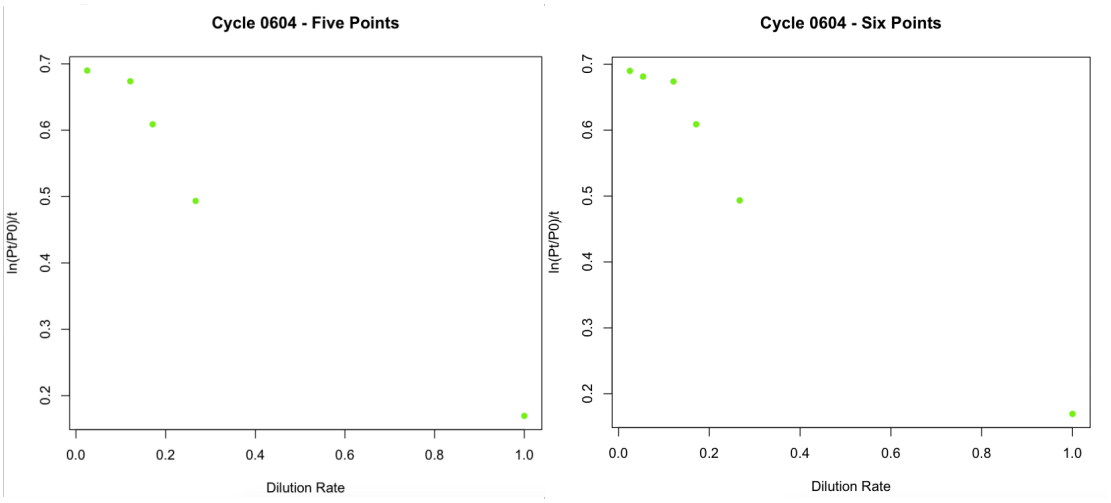

FIGURE 31 – CYCLE 0704 NEW METHOD DILUTION PLOT FOR FIVE AND SIX POINTS

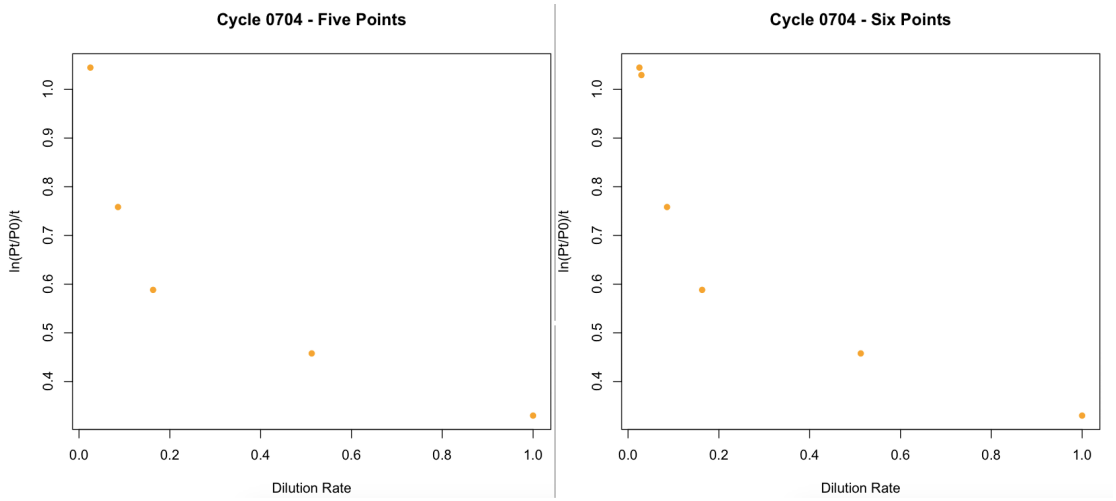

The final results of the method, as well as the nominal difference in error between five and six dilution points, are depicted in Figures 32 and 33 in comparison to the true functional response curve as well as the Li et al. approximation. In fact, the slight increase in the sixth dilution point is difficult to distinguish for cycles 0601 and 0604 while, for cycle 0704, it appears to produce better results when compared to the true response curve in black.

FIGURE 32 – FUNCTIONAL RESPONSES FOR TRUE, APPROXIMATION AND OPTIMAL PARAMETERS

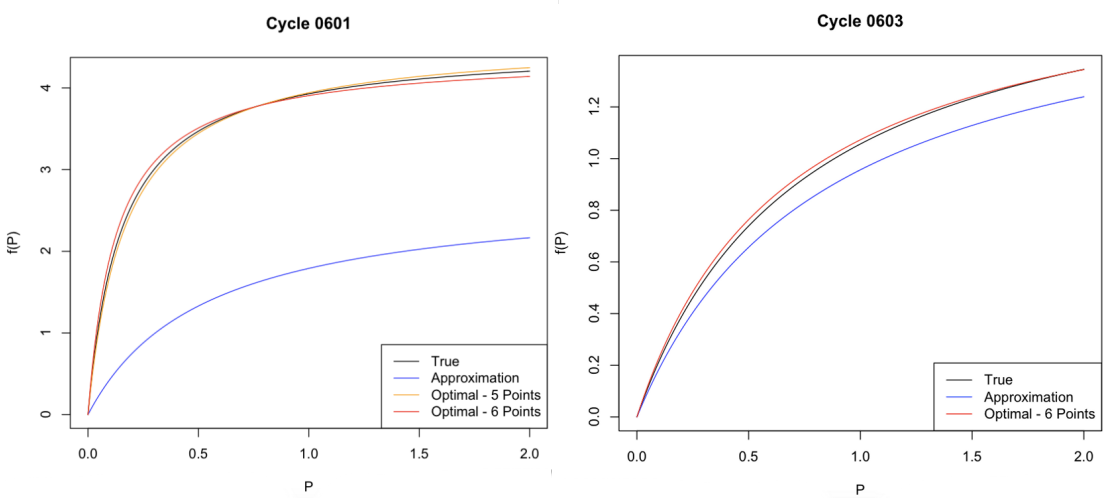

FIGURE 33 – FUNCTIONAL RESPONSES FOR TRUE, APPROXIMATION AND OPTIMAL PARAMETERS

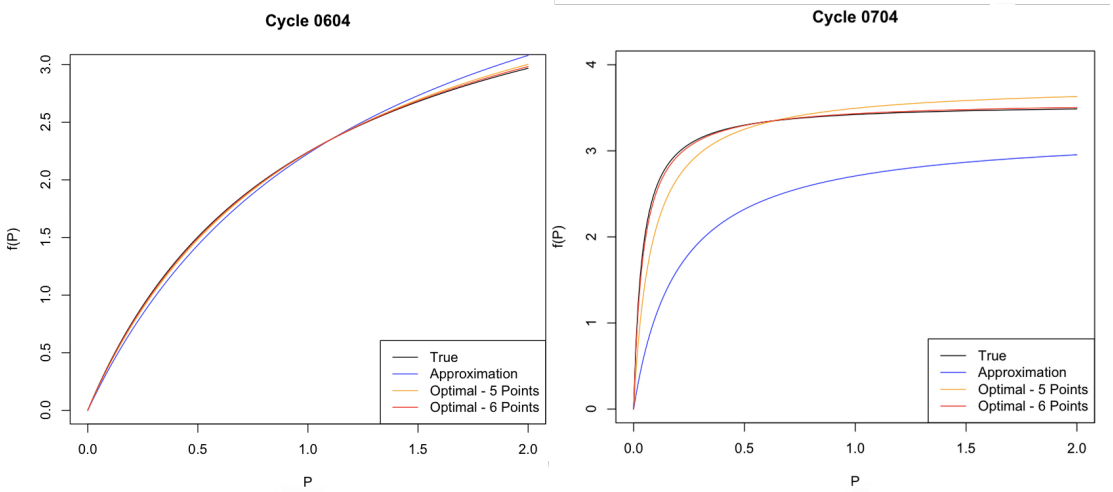

These figures illustrate the promising results of the new method as the optimal curves, with both five and six points, converge closely to the true functional response. However, it does leave room for improvement and hopefully, with refinement, it will prove to be a useful tool in the future.

Chapter 5 – Conclusion

One of the biggest challenges in the ecological modelling of plankton dynamics is the availability of extensive and robust data sets that cover a wide variety of aquatic environments. [10: p.694; 11: p.1304] When considering nonlinear results, that challenge is compounded by the variability within the data collection technique. With options for the number of dilutions and dilution levels ranging from a minimum of 2 to, theoretically, as many as desired, and anywhere between raw seawater and fully diluted respectively, the combinations are extensive. Therefore, it would be beneficial to have some ranges or guidance concerning what combination of dilutions and levels would result in the most accurate estimates.

This research worked to shed some light on optimal dilution levels as well as to offer a new method for approximating the true functional response when it is unknown. In doing so, it was found that the solution of the Holling II differential equation using the 4^{th} order Runge-Kutta method was more advantageous and accurate than an approximation. In examining other functional response curves, it was also discovered that there may be variability in the optimal estimate values for the half-saturation and maximum grazing constants, but their ratio consistently remained the same.

In addition, it was determined that more accurate results occur when the distribution of dilution levels skews towards higher dilution. In terms of optimal dilution allocation, the method of optimisation was sensitive to the initial guess values and therefore, may not be an appropriate measure of the optimal rates. However, the method for approximating the true functional response provided results that were similar to previous tasks as well as being consistent with multiple previous studies.

This research has led me to conclude that, first and foremost, the computational approach is more advantageous, accurate and efficient than other approximation methods and, in capitalising on numerical methods and simulation, greater flexibility was achieved in regard to what could be accomplished within a single computer program. This is clearly visible in the consideration of the additional functional response curves which did not require much additional

computational work. It also reiterated the fact that it is necessary to examine other responses before attempting to finalise a model because small differences may be an unforeseen drawback.

More importantly, though, this research confirmed the need to focus dilution experiments towards higher dilution levels to ensure accurate estimates in the case of both linear and nonlinear responses. The preliminary new method shows promising results consistent with other findings regarding the inclusion of high dilution levels, however, it still requires further development and refinement to improve the consistency and accuracy of the resulting optimal dilution allocations.

Though this research has concluded, there are always ways to improve upon the current methods and models. Therefore, I recommend that the new method is developed further, paying specific attention to sensitivity analysis regarding the noise level of the simulated data and parameter estimates. It also is advisable to experiment with additional constrained optimisation algorithms outside of the interior-point algorithm which may provide better results. The method should also be tested on other functional response curves to determine if the optimal allocation of points is similar regardless of the choice of curve. Finally, I suggest that the new method is utilised to determine the minimum number of dilutions necessary, and the corresponding optimal dilution rates, to maintain minimum error. Hopefully, this will enhance the field experiments employing the dilution technique and provide insight into further plankton model improvements and refinements.

Appendix A

Code 1 – Digitize Data Estimation

```
library(digitize)
read <- ReadAndCal("sixone.jpg")
data <- DigitData(col = "red", type = "p")
Calibrate(data,read,0,1,0,1)
```

Code 2 – Data Simulation

```
function [Pt,r,R] = simdata(f,T,D,P,Q,Z)
%Input: f - function
%       T - time period for solver
%       P - initial phytoplankton biomass
%       D - dilution rate
%       Q - vector containing variables mu, K, g
%       Z - initial zooplankton biomass
%Output: Pt – vector of averaged simulated data with noise
         r – vector of simulated data
          R – matrix of simulated data with noise

n = size(D,2);
m = length(D);

r = opRK4(f,T,D,P,Q,Z); %calculate simulated data

for k = 1:n
    R = zeros(m,n);
    for i = 1:3
        R(1:m,i) = normrnd(r(:,k),(r(:,k)*0.25)/3); %add noise
    end
    M(1:m,k) = mean(R,2); %average noisy data
end
Pt = M;
plot(D,r,'bo',D,Pt,'rx',D,R,'k+') %plot simulated data, noisy
data, and average noisy data
end
```

Code 3 – Runge-Kutta

```
function r = opRK4(f,T,D,P,Q,Z)
%Input: f - ODE function to be solved
%       T - vector including initial and final time and time
step
%       P - initial phytoplankton biomass
%       D - dilution rate
%       Q - vector containing variables mu, K, g
%       Z - initial zooplankton biomass
%Output: net phytoplankton ratio at time t

t = T(1);   tN = T(2);  h = T(3);

N = (tN-t)/h;
P0 = P;     Q0 = Q;
```

```
n1 = length(D);
r = zeros(n1,1);

for j1=1:n1
    for i1=1:N
        k1 = h * f(t,P,D(j1),Q,Z);
        k2 = h * f(t + (h/2),P + (k1/2),D(j1),Q,Z);
        k3 = h * f(t + (h/2),P + (k2/2),D(j1),Q,Z);
        k4 = h * f(t + h,P + k3,D(j1),Q,Z);
        P = P + (k1 + 2*k2 + 2*k3 + k4)/6;
        t = t + h;
    end
    r(j1) = log(P/P0);
    P = P0; Q = Q0;
end
plot(D,r)
end
```

Code 4 – Holling II – Differential Equation

```
function fp = holling2(t,P,D,Q,Z)
%Input: t - time period for solver
%       P - initial phytoplankton biomass
%       D - dilution rate
%       Q - vector containing variables mu, K, g
%       Z - initial zooplankton biomass
%Output: phytoplankton biomass at time t

v = 0;                      %constant net zooplankton growth
rate
u = Q(1);                   %initial phytoplankton growth rate
K = Q(2);                   %half saturation constant
g = Q(3);                   %maximum grazing rate

Z = Z*exp(v*t);             %zooplankton biomass
m = (g*Z)./(K+(D.*P));      %phytoplankton mortality rate
fp = u*P - m*D.*P;
end
```

Code 5 – Holling II – Functional Response

```
function y = h2FRC(P0,Parms)
k = Parms(1);
g = Parms(2);
n = length(P0);
y = zeros(n,1);
for i = 1:n
y(i) = g*((P0(i))/((P0(i)) + k));
end
end
```

Code 6 – Ivlev – Differential Equation

```
function fp = ivlev(t,P,D,Q,Z)
%Input: t - time period for solver
```

```
%       P - initial phytoplankton biomass
%       D - dilution rate
%       Q - vector containing variables mu, K, g
%       Z - initial zooplankton biomass
%Output: phytoplankton biomass at time t

v = 0;                      %constant net zooplankton growth
rate
u = Q(1);                   %initial phytoplankton growth rate
K = Q(2);                   %half saturation constant
g = Q(3);                   %maximum grazing rate

Z = Z*exp(v*t);             %zooplankton biomass
m = (g*(1-exp((-D*P)/K)));  %phytoplankton mortality rate
fp = u*P - m*Z;
end
```

Code 7 – Ivlev – Functional Response

```
function y = ivFRC(P0,Parms)
k = Parms(1);
g = Parms(2);
n = length(P0);
y = zeros(n);
for i = 1:n
y(i) = g*(1 - exp(-P0(i)/k));
end
end
```

Code 8 – Hyperbolic Tangent – Differential Equation

```
function fp = tangent(t,P,D,Q,Z)
%Input: t - time period for solver
%       P - initial phytoplankton biomass
%       D - dilution rate
%       Q - vector containing variables mu, K, g
%       Z - initial zooplankton biomass
%Output: phytoplankton biomass at time t

v = 0;                      %constant net zooplankton growth
rate
u = Q(1);                   %initial phytoplankton growth rate
K = Q(2);                   %half saturation constant
g = Q(3);                   %maximum grazing rate

Z = Z*exp(v*t);             %zooplankton biomass
m = (g*(tanh((D*P)/K)));    %phytoplankton mortality rate
fp = u*P - m*Z;
end
```

Code 9 – Hyperbolic Tangent – Functional Response

```
function y = htFRC(P0,Parms)
k = Parms(1);
g = Parms(2);
n = length(P0);
y = zeros(n);
```

```
for i = 1:n
y(i) = g*tanh(P0(i)/k);
end
end
```

Code 10 – Holling I – Differential Equation

```
function fp = holling1(t,P,D,Q,Z)
%Input: t - time period for solver
%       P - initial phytoplankton biomass
%       D - dilution rate
%       Q - vector containing variables mu, K, g
%       Z - initial zooplankton biomass
%Output: phytoplankton biomass at time t

v = 0;                      %constant net zooplankton growth
rate
u = Q(1);                   %initial phytoplankton growth rate
K = Q(2);                   %half saturation constant
g = Q(3);                   %maximum grazing rate

Z = Z*exp(v*t);             %zooplankton biomass
%m = g*Z;                   %phytoplankton mortality rate
if P < 2*K
    m = (g*D.*P*Z)/(2*K);
else
    m = g*Z;
end
fp = u*P - m;
end
```

Code 11 – Holling I – Functional Response

```
function y = h1 FRC(P0,Parms)
k = Parms(1);
g = Parms(2);
n = length(P0);
y = zeros(n,1);
for i = 1:n
y(i) = (((g*P0(i))/(2*k))*(1/(1 + exp((P0(i) -
(2*k))/0.0001)))) + g*(1/(1 + exp(-(P0(i) - (2*k))/0.0001)));
end
end
```

Code 12 – Optimal Parameters

```
function p = opparm(f,T,D,P,Q,Z,E)
%Input: f - function
%       T - time period for solver
%       P - initial phytoplankton biomass
%       D - dilution rate
%       Q - vector containing variables mu, K, g
%       Z - initial zooplankton biomass
%       E – observed net growth values
%Output: vector of optimal parameters

parhistory.x = [];
```

```
parhistory.fval = [];

options =
optimset('OutputFcn',@myoutput,'MaxFunEvals',100000,'MaxIter',
100000);   %optimisation options
x0 = normrnd(Q(:),(Q(:)*0.15)/3); %initial guess with noise

error = @(f,T,D,P,Q,Z) sum((E - opRK4(f,T,D,P,Q,Z)).^2); %cost
function
[p,fval] = fminsearch(@(i)
error(f,T,D,P,[i(1);i(2);i(3)],Z),x0,options); %optimisation
sse = sum((E-opRK4(f,T,D,P,p,Z)).^2);

    function stop = myoutput(x,optimValues,state) %stores all
optimisation data at each evaluation
    stop = false;

        switch state
            case 'init'
                hold on
            case 'iter'
                parhistory.fval = [parhistory.fval;
optimValues.fval];
                parhistory.x = [parhistory.x x(:)];
            case 'done'
                hold off
            otherwise
        end
    end
end
```

Code 13 – Confidence Intervals

```
f = @(x,xdata) opRK4(fun,[0;1;0.1],xdata,P,x,Z);
[x2,residual2,jacobian2] = lsqcurvefit(fun,[u;K;g],D,E)
[p2,R2,J2] = nlinfit(D,E,fun,[u;K;g])
ci2 = nlparci(p2,R2,'jacobian',J2)

%fun - function
%[u;K;g] — phytoplankton growth, half-saturation, max grazing
guess
%D — observed dilution rates, E — observed net growth rates
```

Code 14 – Optimal Dilution Rates (Version 1)

```
function [D,Pt,Q] = dilutionrate(f,T,D,P,Q,Z)
%Input: f - function
%       T - time period for solver
%       P - initial phytoplankton biomass
%       D — initial dilution rate vector
%       Q - vector containing variables mu, K, g
%       Z - initial zooplankton biomass
%Output: D — vector of optimal dilution rates
%       Pt — associated vector of simulated data with noise
%       Q — associated vector of optimal parameters

objhistory.fval = [];
```

```
objhistory.x = [];
parhistory.fval = [];
parhistory.x = [];
QQ = Q;
Pt = [];

options =
optimoptions(@fmincon,'MaxFunctionEvaluations',500000000,'Outp
utFcn',@outfun); %optimisation options
D0 = normrnd(D(:),(D(:)*0.25)/3); %initial guess
lb = zeros(length(D0),1);  %lower bound
ub = ones(length(D0),1);   %upper bound

    function [c,ceq] = mycon(DR)      %nonlinear constraint
        c = [DR(1) - DR(2);
            DR(2) - DR(3);
            DR(3) - DR(4);
            DR(4) - DR(5)];
         ceq = [];
    end

[DR] = fmincon(@(i)
opsimul(f,T,[i(1);i(2);i(3);i(4);i(5);1],P,Q,Z),D0,[],[],[],[]
,lb,ub,@mycon,options);
D = vertcat(DR(1:5),1);
Q = parhistory.x(:,size(parhistory.x,2));
%plot(D,Pt,'o')
%hold on

    function stop = outfun(x,optimValues,state) %store all
data for all function evaluations
        stop = false;

        switch state
            case 'init'
                hold on
            case 'iter'
                objhistory.fval = [objhistory.fval;
optimValues.fval];
                objhistory.x = [objhistory.x x(:)];
            case 'done'
                hold off
            otherwise
        end
    end

    function err = opsimul(f,T,D,P,Q,Z) %cost function
    Pt = simdata(f,T,D,P,QQ,Z);  %data simulation
    R = opRK4(f,T,D,P,Q,Z);
    plot(D,R,'x')
    pa(:,1) = opparm(f,T,D,P,Q,Z,Pt);  %optimizes parameters
using simulated data with noise
    R = opRK4(f,T,D,P,pa,Z);
    P0 = [0:0.01:2];
    err = abs(trapz(P0,h2FRC(P0,[pa(2);pa(3)])) -
trapz(P0,h2FRC(P0,[QQ(2);QQ(3)])));   %calculates absolute
integral difference calling holling ii functional response
```

```
function
    end

    function p = opparm(f,T,D,P,Q,Z,E)

    options = optimset('OutputFcn',@myoutput);
    x0 = normrnd(Q(:),(Q(:)*0.25)/3);
    error = @(f,T,D,P,Q,Z) sum((E - opRK4(f,T,D,P,Q,Z)).^2);
    [p,fval] = fminsearch(@(i)
error(f,T,D,P,[i(1);i(2);i(3)],Z),x0,options);

        function stop = myoutput(x,optimValues,state)
        stop = false;

            switch state
                case 'init'
                    hold on
                case 'iter'
                    parhistory.fval = [parhistory.fval;
optimValues.fval];
                    parhistory.x = [parhistory.x x(:)];
                case 'done'
                    hold off
                otherwise
            end
        end
    end
    function Pt = simdata(f,T,D,P,Q,Z)

    nn = size(D,2);
    m = length(D);

    r = opRK4(f,T,D,P,Q,Z);

    for kk = 1:nn
        R = zeros(m,nn);
        for ii = 1:3
            R(1:m,ii) = normrnd(r(:,kk),(r(:,kk)*0.25)/3);
        end
        M(1:m,kk) = mean(R,2);
    end
    Pt = M;
    end
end
```

Code 15 – Optimal Dilution Rates (Version 2)

```
function [D,Pt,Q] = dilutionrate2(f,T,D,P,Q,Z)
%Input: f - function
%       T - time period for solver
%       P - initial phytoplankton biomass
%       D – initial dilution rate vector
%       Q - vector containing variables mu, K, g
%       Z - initial zooplankton biomass
%Output: D – vector of optimal dilution rates
%       Pt – associated vector of simulated data with noise
%       Q – associated vector of optimal parameters
```

```
P0 = [0:0.01:2];
objhistory.fval = [];
objhistory.x = [];
parhistory.fval = [];
parhistory.x = [];
QQ = Q;
Pt = [];

options =
optimoptions(@fmincon,'MaxFunctionEvaluations',500000000,'Outp
utFcn',@outfun);%optimisation options
D0 = normrnd(D(:),(D(:)*0.25)/3);     %initial guess
lb = zeros(length(D0),1);  %lower bound
ub = ones(length(D0),1);   %upper bound

    function [c,ceq] = mycon(DR) %nonlinear constraint
        c = [DR(1) - DR(2);
            DR(2) - DR(3);
            DR(3) - DR(4);
            DR(4) - DR(5)];
         ceq = [];
    end

[DR] = fmincon(@(i)
opsimul(f,T,[i(1);i(2);i(3);i(4);i(5);1],P,Q,Z),D0,[],[],[],[]
,lb,ub,@mycon,options);
D = vertcat(DR(1:5),1);
Q = parhistory.x(:,size(parhistory.x,2));
%plot(D,Pt,'o')
%hold on

    function stop = outfun(x,optimValues,state)
        stop = false;

        switch state
            case 'init'
                hold on
            case 'iter'
                objhistory.fval = [objhistory.fval;
optimValues.fval];
                objhistory.x = [objhistory.x x(:)];
            case 'done'
                hold off
            otherwise
        end
    end

    function err = opsimul(f,T,D,P,Q,Z)     %cost function
    Pt = simdata(f,T,D,P,QQ,Z);
    R = opRK4(f,T,D,P,Q,Z);
    plot(D,R,'x')
    pa(:,1) = opparm2(f,T,D,P,Q,Z,Pt);  %optimizes parameters
using simulated data with noise
    R = opRK4(f,T,D,P,pa,Z);
    err = abs(trapz(P0,h2FRC(P0,[pa(2);pa(3)])) -
trapz(P0,h2FRC(P0,[QQ(2);QQ(3)])));   %calculates absolute
```

```
integral difference calling holling ii functional response
function
    end

    function p = opparm2(f,T,D,P,Q,Z,E)

    options = optimoptions(@fmincon,'OutputFcn',@myoutput);
    x0 = normrnd(Q(:),(Q(:)*0.25)/3); %initial guess
    function [c,ceq] = con(p) %parameter nonlinear constraint
                ceq = [];
                c = abs(trapz(P0,h2FRC(P0,[p(2);p(3)])) -
trapz(P0,h2FRC(P0,[QQ(2);QQ(3)]))) -
abs(trapz(P0,h2FRC(P0,[Q(2);Q(3)])) -
trapz(P0,h2FRC(P0,[QQ(2);QQ(3)]))); %calls holling ii
functional response function
    end
    error = @(f,T,D,P,Q,Z) sum((E - opRK4(f,T,D,P,Q,Z)).^2);
      %cost function
    p = fmincon(@(i)
error(f,T,D,P,[i(1);i(2);i(3)],Z),x0,[],[],[],[],[],[],@con,op
tions);

        function stop = myoutput(x,optimValues,state)
        stop = false;

            switch state
                case 'init'
                    hold on
                case 'iter'
                    parhistory.fval = [parhistory.fval;
optimValues.fval];
                    parhistory.x = [parhistory.x x(:)];
                case 'done'
                    hold off
                otherwise
            end
        end
    end
    function Pt = simdata(f,T,D,P,Q,Z)

    nn = size(D,2);
    m = length(D);

    r = opRK4(f,T,D,P,Q,Z);

    for kk = 1:nn
        R = zeros(m,nn);
        for ii = 1:3
            R(1:m,ii) = normrnd(r(:,kk),(r(:,kk)*0.25)/3);
        end
        M(1:m,kk) = mean(R,2);
    end
    Pt = M;
    end
end
```

Code 16 – Optimal Parameter Simulation (Monte Carlo)

```
function [pp,se,ci,sse,p,SSE] = untitled11(f,T,D,P,Q,Z,n)
p = [];
SSE = [];
for k = 1:n
        Pt = simdata(f,T,D,P,Q,Z);
        [pr,sse1] = opparm(f,T,D,P,Q,Z,Pt);
        p = [p pr];
        SSE = [SSE sse1];
end
pp = mean(p,2);
p2 = (bsxfun(@minus,p,pp)).^2;
se = sqrt(sum(p2,2)./(n-1));
ci = se*1.96;
sse = sum((Pt-opRK4(f,T,D,P,pp,Z)).^2);
end
```

Code 17 – New Method

```
function [D,err,Pt,Q,parhistory] = newmethod(f,T,D,P,Q,Z,n)
%Input: f - function
%       T - time period for solver
%       P - initial phytoplankton biomass
%       D – vector of initial fixed dilution rates
%       Q - vector containing variables mu, K, g
%       Z - initial zooplankton biomass
%       n – number of total dilution rates to optimise
%Output: D – vector of optimal dilution rates
%       err – vector of error values
%       Pt – vector of simulated data with noise
%       Q – matrix of optimal parameters

Pt = [];
err = [];
QQ = Q;
P0 = 0:0.01:2;
parhistory.fval = [];
parhistory.x = [];

for i = 1:2
Pt(i,1) = simdata(f,T,D(i),P,Q,Z); %simulated data for fixed
dilution points
end
Q(:,1) = opparm(f,T,D,P,Q,Z,Pt); %optimal parameters for fixed
dilution points

err(1,1) = abs(trapz(P0,h2FRC(P0,[Q(2);Q(3)])) -
trapz(P0,h2FRC(P0,[QQ(2);QQ(3)]))); %absolute integral
difference for fixed dilution points calling holling ii
functional response function

for j = 3:n
    [D,Pt,Q(:,j-1)] = dilutionrate(f,T,D,P,Q(:,j-2),Z,Pt,j);
    plot(D,Pt,'o')
    err(j-1,1) = abs(trapz(P0,h2FRC(P0,[Q(2,j-1);Q(3,j-1)])) -
trapz(P0,h2FRC(P0,[QQ(2);QQ(3)]))); %calls holling ii
```

```
functional response function
end
figure
plot(P0,h2FRC(P0,[QQ(2);QQ(3)]),'k','DisplayName','True')
hold on
for k = 2:n
plot(P0,h2FRC(P0,[Q(2,k-1);Q(3,k-
1)]),'DisplayName',[num2str(k) ' Points'])
end
legend('show','Location','Southeast')

    function [D,Pt,Q] = dilutionrate(f,T,D,P,Q,Z,Pt,n)

    objhistory.fval = [];
    objhistory.x = [];

    options =
optimoptions(@fmincon,'MaxFunctionEvaluations',500000000,'Outp
utFcn',@outfun);
    D0 = mean(D);%normrnd(D(:),(D(:)*0.15)/3);   %initial
guess
    lb = D(1)*ones(length(D0),1);     %lower bound
    ub = ones(length(D0),1);          %upper bound

        function [c,ceq] = mycon(D0)  %nonlinear constraint
            c = D0+0.05 - D(n-1);
            ceq = [];
        end

    DR = fmincon(@(i)
opsimul(f,T,[D;i],P,Q,Z),D0,[],[],[],[],lb,ub,@mycon,options);
    D = vertcat(D,DR);
    Q = parhistory.x(:,size(parhistory.x,2));
    %plot(D,Pt,'o')
    %hold on

        function stop = outfun(x,optimValues,state)
            stop = false;

            switch state
                case 'init'
                    hold on
                case 'iter'
                    objhistory.fval = [objhistory.fval;
optimValues.fval];
                    objhistory.x = [objhistory.x x(:)];
                case 'done'
                    hold off
                otherwise
            end
        end

    function err = opsimul(f,T,D,P,Q,Z)     %cost function
    Pt(n,1) = simdata(f,T,D(n,1),P,QQ,Z);
    R = opRK4(f,T,D,P,Q,Z);
    plot(D,R,'x')
    pa(:,1) = opparm2(f,T,D,P,Q,Z,Pt);  %optimizes parameters
```

```
using simulated data with noise with constraint
    R = opRK4(f,T,D,P,pa,Z);
    err = abs(trapz(P0,h2FRC(P0,[pa(2);pa(3)])) -
trapz(P0,h2FRC(P0,[QQ(2);QQ(3)]))); %calls holling ii
functional response function
    end

    function Pt = simdata(f,T,D,P,Q,Z)

    nn = size(D,2);
    m = length(D);

    r = opRK4(f,T,D,P,Q,Z);

    for kk = 1:nn
        R = zeros(m,nn);
        for ii = 1:3
            R(1:m,ii) = normrnd(r(:,kk),(r(:,kk)*0.25)/3);
        end
        M(1:m,kk) = mean(R,2);
    end
    Pt = M;
    %plot(D,r,'bo',D,Pt,'rx',D,R,'k+')
    end

    function p = opparm2(f,T,D,P,Q,Z,E)

    options = optimoptions(@fmincon,'OutputFcn',@myoutput);
    x0 = normrnd(Q(:),(Q(:)*0.25)/3); %initial guess
    function [c,ceq] = con(p)    %nonlinear constraint
                ceq = [];
                c = abs(trapz(P0,h2FRC(P0,[p(2);p(3)])) -
trapz(P0,h2FRC(P0,[QQ(2);QQ(3)]))) -
abs(trapz(P0,h2FRC(P0,[Q(2);Q(3)])) -
trapz(P0,h2FRC(P0,[QQ(2);QQ(3)]))); %calls holling ii
functional response function
    end
    error = @(f,T,D,P,Q,Z) sum((E - opRK4(f,T,D,P,Q,Z)).^2);
      %cost function
    p = fmincon(@(i)
error(f,T,D,P,[i(1);i(2);i(3)],Z),x0,[],[],[],[],[],[],@con,op
tions);

        function stop = myoutput(x,optimValues,state)
        stop = false;

            switch state
                case 'init'
                    hold on
                case 'iter'
                    parhistory.fval = [parhistory.fval;
optimValues.fval];
                    parhistory.x = [parhistory.x x(:)];
                case 'done'
                    hold off
                otherwise
            end
```

```
        end
    end
end
end
```

Appendix B

TABLE B1 – CALCULATIONS FOR MAXIMUM GRAZING RATE

$\frac{dP}{dt} = P(\mu - m) = \mu P - mP$	
$\frac{dP}{dt} = \mu P - g_{max} f(P) Z$	
$\mu P - mP = \mu P - g_{max} f(P) Z$	
$mP = g_{max} f(P) Z$	
Holling II	Ivlev
$f(P) = \frac{P}{K + P}$	$f(P) = (1 - e^{-P/K})$
$mP = g_{max} \frac{P}{K + P} Z$	$mP = g_{max}(1 - e^{-P/K}) Z$
$m = g_{max} \frac{Z}{K + P}$	$m = \frac{1}{P} g_{max}(1 - e^{-P/K}) Z$
Hyperbolic Tangent	Holling I
$f(P) = \tanh \frac{P}{K}$	$f(P) = \begin{cases} \frac{P}{2K}, & P < 2K \\ 1, & P \geq 2K \end{cases}$
$mP = g_{max} \tanh \frac{P}{K} Z$	$mP = g_{max} Z \begin{cases} \frac{P}{2K}, & P < 2K \\ 1, & P \geq 2K \end{cases}$
$m = \frac{1}{P} g_{max} \tanh \frac{P}{K} Z$	$m = \frac{1}{P} g_{max} Z \begin{cases} \frac{P}{2K}, & P < 2K \\ 1, & P \geq 2K \end{cases}$

Appendix C

TABLE C1 – LI ET AL. APPROXIMATION PARAMETER ESTIMATES

Cycle	0601	0603	0604	0704
P_0	2.68 ± 0.21	3.29 ± 0.22	0.69 ± 0.08	0.43 ± 0.04
Z_0	0.75 ± 0.16	1.20 ± 0.89	0.22 ± 0.02	0.13 ± 0.05
μ	0.90 ± 0.17	0.64 ± 0.03	0.72 ± 0.01	0.92 ± 0.02
$\overline{m}$	0.64 ± 0.16	0.51 ± 0.02	0.57 ± 0.01	0.67 ± 0.02
K	0.53 ± 0.38	0.84 ± 0.37	1.24 ± 0.12	0.20 ± 0.08

TABLE C2 – APPROXIMATED DATA FROM LI ET AL. DILUTION PLOTS

Cycle 0601		Cycle 0603		Cycle 0604		Cycle 0704	
Dilution Rate	Net Growth Rate	Dilution Rate	Net Growth Rate	Dilution Rate	Net Growth Rate	Dilution Rate	Net Growth Rate
0.2283	0.5758	0.0184	0.7376	0.0418	0.7512	0.0805	0.8652
0.2277	0.4236	0.0191	0.4726	0.0412	0.6361	0.0802	0.8022
0.4459	0.4044	0.0835	0.6429	0.2274	0.5774	0.0806	0.7133
0.4468	0.3530	0.0834	0.2996	0.2302	0.4993	0.2128	0.5993
0.6388	0.3334	0.2287	0.3896	0.4693	0.3957	0.2043	0.5123
0.6398	0.2417	0.2291	0.2982	0.4664	0.4020	0.3942	0.5786
0.8516	0.3729	0.4692	0.3502	0.6527	0.3493	0.3959	0.4833
0.8525	0.3322	0.4673	0.1481	0.6511	0.2347	0.5894	0.3386
1.0000	0.3346	0.6535	0.0269	0.8541	0.2859	0.8090	0.3464
1.0000	0.3016	0.6534	0.2983	0.8567	0.2261	0.8050	0.3490
1.0000	0.2555	0.8585	0.2120	1.0000	0.2049	1.0000	0.2095
1.0000	0.2039	0.8575	0.0822	1.0000	0.2024	1.0000	0.5128
1.0000	0.1914	1.0000	-0.0123	1.0000	0.1864		
		1.0000	-0.1029	1.0000	0.0245		

TABLE C3 – STANDARD ERROR AND CONFIDENCE INTERVALS FOR CYCLE 0603

Cycle 0603				
Holling II	**Parameter Estimate**	**Standard Error**	**Confidence Interval**	
μ	0.6506	0.1379	0.3387	0.9625
K	0.7529	1.0652	-1.6568	3.1626
g_{max}	1.8518	0.4728	0.7821	2.9214
Ivlev	**Parameter Estimate**	**Standard Error**	**Confidence Interval**	
μ	0.6256	0.1067	0.3843	0.8670
K	0.9027	0.7549	-0.8050	2.6105
g_{max}	1.4470	0.3227	0.7172	2.1770
Tangent	**Parameter Estimate**	**Standard Error**	**Confidence Interval**	

μ	0.6070	0.0958	0.3904	0.8237
K	1.2382	0.8064	-0.5860	3.0624
g_{max}	1.3504	0.3010	0.6695	2.0313
Holling I	**Parameter Estimate**	**Standard Error**	**Confidence Interval**	
μ	0.5277	6.63e-05	0.5276	0.5279
K	2.7634	48.1410	-91.5923	97.1203
g_{max}	2.3658	41.1454	-78.2790	83.0107

TABLE C4 – STANDARD ERROR AND CONFIDENCE INTERVALS FOR CYCLE 0604

Cycle 0604				
Holling II	**Parameter Estimate**	**Standard Error**	**Confidence Interval**	
μ	0.7316	0.0569	0.6063	0.8569
K	0.9589	0.9063	-1.0357	2.9536
g_{max}	4.3921	2.1324	-0.3014	9.0855
Ivlev	**Parameter Estimate**	**Standard Error**	**Confidence Interval**	
μ	0.7275	0.0531	0.6107	0.8443
K	0.6713	0.4867	-0.3998	1.7425
g_{max}	2.8428	1.0286	0.5790	5.1067
Tangent	**Parameter Estimate**	**Standard Error**	**Confidence Interval**	
μ	0.7176	0.0481	0.6117	0.8235
K	0.6804	0.3040	0.0115	1.3494
g_{max}	2.3406	0.4892	1.2638	3.4173
Holling I	**Parameter Estimate**	**Standard Error**	**Confidence Interval**	
μ	0.6761	4.05e-05	0.6760	0.6762
K	0.6751	4.5501	-8.2432	9.5934
g_{max}	3.2449	21.8339	-39.5496	46.0395

TABLE C5 – STANDARD ERROR AND CONFIDENCE INTERVALS FOR CYCLE 0704

Cycle 0704				
Holling II	**Parameter Estimate**	**Standard Error**	**Confidence Interval**	
μ	1.2067	0.5636	-0.0682	2.4815
K	0.0388	0.0690	-0.1172	0.1948
g_{max}	3.5547	1.7588	-0.4239	7.5333
Ivlev	**Parameter Estimate**	**Standard Error**	**Confidence Interval**	
μ	0.9688	0.1431	0.6452	1.2925
K	0.1081	0.0568	-0.0204	0.2366
g_{max}	2.4129	0.4699	1.3500	3.4758
Tangent	**Parameter Estimate**	**Standard Error**	**Confidence Interval**	

μ	0.9106	0.1092	0.6636	1.1577
K	0.1686	0.0697	0.0109	0.3262
g_{max}	2.1726	0.3844	1.3031	3.0422
Holling I	**Parameter Estimate**	**Standard Error**	**Confidence Interval**	
μ	0.7422	8.84e-05	0.7420	0.7424
K	0.4383	5.0009	-9.3634	10.2400
g_{max}	3.0975	35.6776	-66.8306	73.0257

TABLE C6 – ALTERNATIVE OPTIMAL PARAMETERS FOR CYCLE 0603

Cycle 0603		Differential Optimal Parameters			
		Holling II	Ivlev	Tangent	Holling I
Given Parameters	P_0	3.2900	3.2900	3.2900	3.2900
	Z_0	1.2000	1.2000	1.2000	1.2000
Estimated Parameters	μ	0.6120	0.5923	0.5748	0.5297
	K	1.7198	1.7683	2.2495	2.9674
	g_{max}	2.3543	1.7743	1.6151	2.5821
Sum of Squares		0.1810	0.1838	0.1882	0.2004

TABLE C7 – ALTERNATIVE STANDARD ERROR AND CONFIDENCE INTERVALS FOR CYCLE 0603

Differential Equation – Cycle 0603				
Holling II	**Parameter Estimate**	**Standard Error**	**Confidence Interval**	
μ	0.6120	0.1007	0.3903	0.8337
K	1.7196	2.1989	-3.1201	6.5594
g_{max}	2.3542	0.9243	0.3198	4.3887
Ivlev	**Parameter Estimate**	**Standard Error**	**Confidence Interval**	
μ	0.5923	0.0864	0.4022	0.7825
K	1.7682	1.6504	-1.8644	5.4008
g_{max}	1.7743	0.5751	0.5086	3.0400
Tangent	**Parameter Estimate**	**Standard Error**	**Confidence Interval**	
μ	0.5748	0.0781	0.4029	0.7467
K	2.2493	1.5190	-1.0941	5.5926
g_{max}	1.6150	0.4187	0.6934	2.5366
	Parameter Estimate	**Standard Error**	**Confidence Interval**	
μ	0.5297	6.63e-05	0.5296	0.5299
K	2.9674	40.1061	-75.6406	81.5754
g_{max}	2.5821	37.4801	-70.8789	76.0431

References

1. May R.M. *Theoretical Ecology: Principles and Applications*. 2nd Ed. Oxford: Blackwell Scientific Publications; 1981.
2. Yang Xin-She. *Mathematical Modelling for Earth Sciences* [Internet]. Edinburgh: Dunedin Academic Press; 2008. [cited 2017 August 1]. Available from: ProQuest Ebook Central.
3. Falkowski P. Ocean Science: The Power of Plankton. *Nature* [Internet]. 2012 [cited 2017 August 2]; 483(7387). Available from: doi: 10.1038/483S17a.
4. Brierley, A.S. Plankton. *Current Biology* [Internet]. 2017 June 5 [cited 2017 August 2]; 27(11): R478-R510. Available from: doi: 10.1016/j.cub.2017.02.045.
5. Holling CS. Some Characteristics of Simple Types of Predation and Parasitism. *The Canadian Entomologist*. 1959 July; 91(07):385–98. Available from: doi: 10.4039/ent91385-7.
6. Landry MR, Hassett RP. Estimating the grazing impact of marine micro-zooplankton. *Marine Biology* [Internet]. 1982; 67(3):283–8. Available from: doi: 10.1007/bf00397668.
7. Gentleman W. A chronology of plankton dynamics in silico: how computer models have been used to study marine ecosystems. *Hydrobiologia* [Internet]. 2002 July; 480(1-3):69–85. Available from: doi: 10.1023/A:1021289119442.
8. U. Illustration of a microbial loop. [Internet]. Microbial Loop. Wikipedia; 2006. Available from: https://en.wikipedia.org/wiki/Microbial_loop.
9. Li Q. P., Franks P. J. S., Landry M. R. Recovering growth and grazing rates from nonlinear dilution experiments. *Limnology and Oceanography* [Internet]. 2017; Available from: doi: 10.1002/lno.10536.
10. Shmoker C, Hernández-León S, Calbet A. Microzooplankton grazing in the oceans: impacts, data variability, knowledge gaps and future directions, *Journal of Plankton Research* [Internet]. 2013 July 1; 35(4): 691–706. Available from: doi: 10.1093/plankt/fbt023.
11. Franks, P.J.S. Planktonic Ecosystem Models: Perplexing Parameterizations and a Failure to Fail. *Journal of Plankton Research* [Internet]. 2009 December [cited 2017 August 2]; 31(11): 1299-306. Available from: doi: 10.1093/plankt/fbp069.
12. Britton N.F. *Essential Mathematical Biology*. London: Springer; 2003.
13. Moigis A-G. The clearance rate of microzooplankton as the key element for describing estimated non-linear dilution plots demonstrated by a model. *Marine Biology* [Internet]. 2006 August; 149(4):743–62. Available from: doi: 10.1007/s00227-005-0202-3.
14. Gallegos C. Microzooplankton grazing on phytoplankton in Rhode River, Maryland: nonlinear feeding kinetics. *Marine Ecology Progress Series* [Internet]. 1989 September 15; 57:23–33. Available from: doi: 10.3354/meps057023.

15. Evans G, Paranjape M. Precision of estimates of phytoplankton growth and microzooplankton grazing when the functional response of grazers may be nonlinear. *Marine Ecology Progress Series* [Internet]. 1992 March 3; 80:285–90. Available from: doi: 10.3354/meps080285.
16. Landry M, Kirshtein J, Constantinou J. A refined dilution technique for measuring the community grazing impact of microzooplankton, with experimental tests in the central equatorial Pacific. *Marine Ecology Progress Series* [Internet]. 1995 April 20; 120:53–63. Available from: doi: 10.3354/meps120053.
17. Gallegos CL, Vant WN, Safi KA. Microzooplankton grazing of phytoplankton in Manukau Harbour, New Zealand. *New Zealand Journal of Marine and Freshwater Research* [Internet]. 1996; 30(4):423-434. Available from: doi: 10.1080/00288330.1996.9516730.
18. Dolan J, Gallegos C, Moigis A. Dilution effects on microzooplankton in dilution grazing experiments. *Marine Ecology Progress Series* [Internet]. 2000 July 14; 200:127–39. Available from: doi: 10.3354/meps200127.
19. Worden A, Binder B. Application of dilution experiments for measuring growth and mortality rates among Prochlorococcus and Synechococcus populations in oligotrophic environments. *Aquatic Microbial Ecology* [Internet]. 2003 January 7; 30:159–74. Available from: doi: 10.3354/ame030159.
20. Teixeira I, Figueiras F. Feeding behaviour and non-linear responses in dilution experiments in a coastal upwelling system. *Aquatic Microbial Ecology* [Internet]. 2009 January; 55:53–63. Available from: doi: 10.3354/ame01281.
21. Sanderson BG, Redden AM, Evans K. Grazing Constants are Not Constant: Microzooplankton Grazing is a Function of Phytoplankton Production in an Australian Lagoon. *Estuaries and Coasts* [Internet]. 2012; 35(5):1270–84. Available from: doi: 10.1007/s12237-012-9524-9.
22. Chen B, Laws EA, Liu H, Huang B. Estimating microzooplankton grazing half-saturation constants from dilution experiments with nonlinear feeding kinetics. *Limnology and Oceanography* [Internet]. 2014 April 7; 59(3):639–44. Available from: doi: 10.4319/lo.2014.59.3.0639.
23. Chen B. Assessing the accuracy of the "two-point" dilution technique. *Limnology and Oceanography: Methods* [Internet]. 2015 June 4; 13:521–526. Available from: doi:10.1002/lom3.10044.
24. Redden A, Sanderson B, Rissik D. Extending the analysis of the dilution method to obtain the phytoplankton concentration at which microzooplankton grazing becomes saturated. *Marine Ecology Progress Series* [Internet]. 2002 January 31; 226:27–33. Available from: doi: 10.3354/meps226027.
25. Li Q, Franks P, Landry M. Microzooplankton grazing dynamics: - parameterizing grazing models with dilution experiment data from the

California Current Ecosystem. *Marine Ecology Progress Series* [Internet]. 2011 October 5; 438:59–69. Available from: doi: 10.3354/meps09320.
26. Poisot TCA, Sachse R, Ashander J, Galili T. *Package 'digitize'* [Internet]. 2016. Available from: https://cran.r-project.org/web/packages/digitize/digitize.pdf.
27. Weisstein EW. *Standard Deviation* [Internet]. From MathWorld--A Wolfram Web Resource. [cited 2017 September 2]. Available from: MathWorld.
28. *Module 1: Numerical Solution of Ordinary Differential Equations* [Internet]. Course: Numerical Solution of Ordinary Differential Equations. Available from: http://nptel.ac.in/courses/111107063/module1/lecture1/lecture1.pdf.
29. Logan JD. *A First Course in Differential Equations* [Internet]. New York: Springer; 2011. Available from: SpringerLink.
30. Pav SE. *Numerical Methods Course Notes, Version 0.11*. 2005. Available from: Blackboard.
31. Griffiths DF, Higham DJ. *Numerical methods for ordinary differential equations: initial value problems* [Internet]. London: Springer; 2011. Available from: SpringerLink.
32. Allaire, Grégoire. *Numerical Analysis and Optimisation: An Introduction to Mathematical Modelling and Numerical Simulation* [Internet]. Oxford: OUP Oxford; 2007. [cited 2017 August 4]. Available from: ProQuest Ebook Central.
33. Berg Hvan den. *Mathematical models of biological systems*. Oxford: Oxford University Press; 2011.
34. MathWorks United Kingdom. *Find minimum of unconstrained multivariable function using derivative-free method - MATLAB fminsearch* [Internet]. Documentation. [cited 2017 September 1]. Available from: MathWorks.
35. Press WH. *Numerical recipes in C*. Cambridge: Cambridge Univ. Press; 2002.
36. Hendrix EMT, G.-Tóth Boglárka. *Introduction to Nonlinear and Global Optimization* [Internet]. New York, NY: Springer New York; 2010. Available from: SpringerLink.
37. MathWorks United Kingdom. *Nonlinear regression - MATLAB nlinfit* [Internet]. Documentation. [cited 2017 September 3]. Available from: MathWorks.
38. MathWorks United Kingdom. *Nonlinear regression parameter confidence intervals - MATLAB nlparci* [Internet]. Documentation. [cited 2017 September 3]. Available from: MathWorks.
39. Motulsky H, Christopoulos A. *Fitting models to biological data using linear and nonlinear regression: a practical guide to curve fitting*. Oxford: Oxford Univ. Press; 2010.
40. MathWorks United Kingdom. *Find minimum of constrained nonlinear multivariable function - MATLAB fmincon* [Internet]. Documentation. [cited 2017 September 1]. Available from: MathWorks.

41. MathWorks United Kingdom. *Constrained Nonlinear Optimization Algorithms* [Internet]. Documentation. [cited 2017 September 1]. Available from: MathWorks.
42. MathWorks United Kingdom. *Trapezoidal numerical integration - MATLAB trapz* [Internet]. Documentation. [cited 2017 September 2]. Available from: MathWorks.